Kuo, Jeng-Chung

LASER-BASED OPTICAL ACTIVITY DETECTOR FOR HIGH PERFORMANCE LIQUID CHROMATOGRAPHY

Iowa State University PH.D. 1982

Laser-based optical activity detector for high performance liquid chromatography

by

Jeng-Chung Kuo

A Dissertation Submitted to the
Graduate Faculty in Partial Fulfillment of the
Requirements for the Degree of
DOCTOR OF PHILOSOPHY

Department: Chemistry
Major: Analytical Chemistry

Approved:

Signature was redacted for privacy.

In Charge of Major Work

Signature was redacted for privacy.

For the Major Department

Signature was redacted for privacy.

For the Graduate College

Iowa State University
Ames, Iowa

1982

TABLE OF CONTENTS

CHAPTER I. INTRODUCTION

Statement of Problem

The combination of liquid chromatography with spectroscopic measurements is one of the most powerful tools available to chemists in the area of chemical analysis today. The coupling of these two techniques, i.e., separation and spectroscopy, produces results which neither technique can provide alone: liquid chromatography is the technique of choice for the separation of thermally unstable, nonvolatile organic and inorganic compounds, and spectroscopy provides both confirmation that separation has taken place and positive identification of the separated compounds as the basis of quantitative evaluation.

When confronted with multicomponent, real-world samples obtained from biological, environmental, or geological sources, the determination of organics by liquid chromatographic methods is often made difficult not only by problems from separation but also by problems from detection. Obviously, if a sample contains many constituents and not all of them are well-separated by HPLC due to lack of resolution, the resulting chromatogram is often a complex maze of peaks if monitored by a nondiscriminating detector.

In the chromatographic separation, the heart of a chromatograph is the column where the interactions between

sample, stationary phase and mobile phase take place. The ultimate goal is to separate components of a sample within a reasonable period of time into distinct bands or peaks as they migrate through the column. When faced with the problem of improving resolution, it is clear that one should first examine the efficiency of the column.

Microparticulate packings with surface-reacted, chemically-bonded, organic stationary phases are very widely used for modern high performance liquid chromatography (HPLC), accounting for some 75% of all current separations (1). Commercially available analytical-scale HPLC columns have, in general, been configured with 4.6-mm i.d. and 250-mm length. When packed with 10-μm spherical particles, a LC column with efficiencies in the order of 40,000 theoretical plates/meter still can not match the separating power of capillary column gas chromatography. Even with the most recent improvements in the resolving power, with theoretical plates in the hundreds of thousands (as with the liquid chromatography microcolumn (2, 3), the lengthy analysis times of between a few hours and a couple of days would render this current development of very limited utility for practical applications at the present stage.

On the detection front, the evolution of modern liquid chromatography from the separation of compounds in the form

of colored rings of earlier days into a major analytical technique now is also helped tremendously by the advancements in the field of optical flowthrough HPLC detectors. Meaningful chromatographic results can be obtained only after the eluting components can be detected and the detector response analyzed. It is suggested (4) that the solution to the problem of peak identification and the elimination of interference from unresolved peaks can be partially provided by employing detectors which respond selectively to the characteristic molecular properties of certain classes of compounds. Selective detection has two basic advantages: first, it gives some information to assist in the identification of the individual compounds present in the sample. In addition, in situations where compounds co-elute (i.e., they could not be separated chromatographically), selective detectors may offer optical separation by permitting the detection of one compound while disregarding the others (5).

Since detectors play such an important role in this analytical process, a brief review and evaluation of current optical detector technology will be presented in the following section.

Review of HPLC Optical Detectors

It is generally agreed that detectors are the weakest link in the liquid chromatographic system. The characteristics of an ideal LC detector are many (1, 6, 7), but no present available detector possesses all the desired properties. The important characteristics which need to be considered when evaluating a detector may be summarized as follows. An LC detector should: (1) have high sensitivity and predictable response to all compounds (except those composing the mobile phase) or show predictable selectivity; (2) show no mobile phase response and be relatively insensitive to variations in mobile phase flow-rate, temperature and composition; (3) have a wide range of linearity, so the quantitative analysis may be accomplished in a straightforward manner; (4) have a fast response time so as to faithfully record fast eluting peaks; (5) provide some information to assist compound identification; (6) be nondestructive to the eluting compounds; (7) not contribute to extracolumn band-broadening, and (8) be easy to operate, reliable, and inexpensive. Obviously, the LC equivalent to the sensitive, universal thermal conductivity and flame ionization detectors of gas chromatography has not yet been produced.

Currently available commercial LC detectors are based

on a number of detection principles, including absorbance, fluorescence, refractive index detection, electrochemical detection and mass spectrometry. A detailed review of this topic will be beyond the scope of this section. However, in addition to the coverage of detectors in the standard LC books (1, 7, 8, 9), some short, concise general overviews (6, 10) and more extensive reviews (11, 12) are readily available.

A survey of scientific papers to find out which detectors were most popular was conducted recently (10). The results show that, by far, optical detection prevails. Overall, it was utilized in more than 90% of the papers surveyed with absorbance detection most widely used. Although optical detectors based on absorbance, fluorescence and refractive index are the current workhorses of LC, they are not without limitations and drawbacks. Absorbance detectors have been the most popular and successful, but generally require the presence of chromophores in compounds to provide suitable absorption bands. This meant that only unsaturated compounds are detectable. A spectrophotometric detector, which can be set to any wavelength from 190 to 700 nm in the UV and visible regions of the spectrum, is sensitive and somewhat selective depending upon the wavelength chosen. But the possible choice of chromatographic

mobile phases is severely limited if the selected wavelength lies in the far-UV side. Typically, fluorescence sensitivity is 100 to 1000 times higher than that of absorbance detection due to the low backgrounds. It also offers a high degree of selectivity because most compounds absorb but relatively few of them fluorescence. But the fact that only a limited number of organic compounds exhibit this phenomenon hinders the wider applicability of fluorescence detection.

Naturally, one can use chemical derivatization, either by a pre- or post-column method, to enhance detector sensitivity and selectivity as well as improve chromatographic behavior. However, ideal derivatization is hard to achieve and the removal of side products and excessive derivatizing agent (13) introduces extra inconvenience. Also, if the availability of samples is a major concern, the destructive nature of the derivatization process will pose a serious problem.

A refractive index (RI) detector, with the mobile phase as a reference, responds to all compounds whose solutions have refractive indices different from solvent after elution from the LC column. Its limitations are poor sensitivity, lack of selectivity, and its sensitivity to temperature and flow changes. To be considered chromatographically significant, a sensitivity better than 10^{-6} RI units is needed. A

typical organic liquid used as mobile phase will undergo a change of 600×10^{-6} RI units with a 1°C temperature variation. Against this temperature effect, a stability of $\pm$ 0.01°C is usually required for high sensitivity operation. Flow programming as well as gradient elution is almost impossible because of the constant changes in refractive index.

The mass spectrometer shows great promise in functioning as an unexcelled, universal and highly specific detector for LC. Considerable effort has been made in recent years to develop an interface capable of coupling the instruments in HPLC-MS (14, 15). In all cases, the performance of various interfaces was less than ideal. The major obstacle has always been the fundamental mismatch between LC flow rate and the vacuum requirements of the mass spectrometer. Channeling the solvent flow from a typical liquid chromatography directly into a mass spectrometer would, after vaporization, produce a gas flow rate which is far greater than the ability of an average mass spectrometer to handle and still maintain a vacuum requirement of 10^{-5} torr or better in the mass analyzer. Although the advancement made in interfacing technique is substantial, this problem is far from being resolved.

Infrared absorbance spectra are very characteristic for

particular organic compounds. For HPLC detection, a high degree of specificity can be achieved if suitable absorbance wavelengths can be chosen to match the organic functional groups of the compounds of interest. In theory, infrared detectors are similar to UV absorbance detectors, only they use an IR light source, but in practice, infrared detectors are severely limited. Although the lack of sensitivity due to a low extinction coefficient of infrared absorption may possibly be overcome through the use of Fourier transform techniques (16), the choice of eluents presents a major problem for the infrared detector. It is necessary to choose mobile phases which are transparent in the infrared region of interest. This makes reversed-phase or ion-exchange chromatography difficult because of the compatibility problem with the OH-containing solvent groups which absorb strongly.

The need for sensitive and selective HPLC detectors is therefore obvious, especially those that are based on entirely different physical or chemical properties that are normally associated with standard instrumentation.

Analytical Approach

The rotation of polarized light by optically active molecules has resulted in relatively few applications in chemical analysis. Accurate determination of the optical rotary power of a sample can provide information regarding its isomeric purity, and can be used for quality control in pharmacological and food-related industries (17). At the same time, since conformation is so specific a property for biological processes, there exist a large number of environmental and clinical systems where optically active species are the most important ones.

An HPLC detector based on optical activity seems to possess many advantages in the problematic area of organic analysis. Since most chromatographic eluents are not optically active, one will not be limited in the choice of eluents or gradients. Such a detector is extremely selective, so that complex samples can be handled. The availability of a sensitive micropolarimeter will therefore benefit organic analysis when coupled to HPLC, and will broaden the applicability of spectropolarimetry in general.

The major object of the research presented in this dissertation is to demonstrate, with examples in the biological and environmental fields, a working, highly sensitive and highly selective laser-based optical activity

detector for HPLC.

A detailed description of the experimental system will be given in Chapter III, after a brief review of various HPLC detectors that are based on lasers is presented in Chapter II, since it is the key to the success. In the chapters that follow, laser optical activity detection coupled with HPLC separation will be applied to (i) the determination of carbohydrates in human urine (Chapter IV), (ii) the determination of free and esterified cholesterol in human serum (Chapter V), and (iii) the characterization of the saturate fractions of various shale oil samples (Chapter VI).

CHAPTER II. REVIEW OF LASER-BASED DETECTORS FOR HIGH PERFORMANCE LIQUID CHROMATOGRAPHY

Introduction

Lasers are sources of coherent light, characterized by a high degree of monochromaticity, high directionality and high intensity or brightness. Since the first working ruby laser was constructed in 1960, lasers are now entering their third decade of existence. With the development of various types of lasers, the stage was set for a rapid evolution for the study in chemistry, physics, biology, medicine, material technology and especially in the field of communications and information processing. The laser is basically a spectroscopic device and most of its properties and operations are well-suited for probing and exploring fundamental atomic and molecular processes (18, 19). Some indication can be obtained from the proceedings of the five biennial conferences on laser spectroscopy (20, 21). In a recent Report feature article (22), some of the major analytical spectroscopic techniques which have benefitted from the utilization of the laser are reviewed at great length. It is fascinating and rewarding, also very challenging to add the laser to the analytical chemist's arsenal of instruments. The analytical uses of the laser include absorption, fluorescence, photoionization, Raman spectroscopy, mass

spectrometry as well as photoacoustic and optogalvanic detection which have been extensively reviewed (23, 24). Texts devoted to analytical laser spectroscopy, containing types and characteristics of lasers, principles of operation, optics and instrumentation and their diverse and burgeoning analytical applications, are also available (25, 26).

Although limited in scope, significant progress is also being made in linking liquid chromatographic systems with the laser. It is appropriate at this point to examine those aspects of laser light which are unique and which make it so attractive as an analytical tool.

Perhaps the most arresting property of laser light is its directionality which is due to the low beam diversion. The laser beam is easily manipulated around an experimental set-up. This offers a number of advantages in designing and carrying out experiments. For example, a highly collimated laser beam over a very long path length cell can increase sensitivity in some absorption measurements. It is also routine to have visible lasers whose wavelength is known to the nearest 0.01 Å and infrared diode lasers with a resolution of 10^{-5} cm^{-1}. The monochromaticity of laser light makes it possible to deposit a precisely known amount of energy into a specific region of an atomic or molecular system. The narrow spectral line-width effectively eliminates the need for monochromators and stray light can be signifi-

cantly reduced by the simple application of laser line filters. Other benefits include selective excitation and reduced spectral interference as demonstrated in wavelength modulation techniques. From an analytical point of view, the large photon fluxes associated with high laser powers (1 W of 500 nm radiation provides 10^{18} photons/sec) enable the detection of extremely small amounts of materials as a result of very favorable shot noise response. It is also a well-known fact that the availability of the high output power of lasers has opened up the field of nonlinear spectroscopic excitation such as multiphoton absorption for analytical applications.

Below, several recent developments in the area of laser-based HPLC detectors will be briefly summarized. For a more detailed discussion the reader is referred to the two authoritative review articles specifically devoted to this subject (27, 28).

Review of Laser-Based HPLC Detectors

The intensity of a fluorescent emission signal is linearly dependent on the number of photons put out by the excitation radiation before saturation effects take place. The popularity of using lasers as the excitation sources for fluorometry stems from the increased photon flux of the laser and the ease of focusing the light beam into

the very small detection volume required for HPLC detectors. More importantly, the monochromatic radiation reduces the bandwidth of Rayleigh and Raman scattering to 1 nm and frees available "windows" for both wavelength discrimination and stray light rejection in fluorescence detection (28).

In the laser-based fluorometric HPLC detector devised by Diebold and Zare (29), the modulated He-Cd laser at 325 nm was focused into a interaction region of less than 3 µl inside the flowing droplet to generate visible fluorescence. The fluorescence from the nonexistent cell walls is thus eliminated and the light scattering significantly reduced. By using proper derivatization, the picogram level determination of aflatoxins B_2, B_{2A}, G_2 and G_{2A} was achieved. The same principles were extended to the fluorometric detection of insuline in enzyme immunoassay (30). An impressive sensitivity of 46 pg/ml was reached.

Some problems that might plague the laminar-flow condition of a flowing droplet windowless sample cell can be effectively corrected by employing a different design based on fiber optics (31). Here the HPLC effluent moved upward into the optical fiber inside a quartz capillary tube cell of 20 µl volume. In addition to the easier optical alignment and better photon collection efficiency, the problems of trapped gas bubbles, gradient elution and thermal lens effect become less severe. Argon ion laser

operated at 488 nm is used as the excitation source for the generation of visible fluorescence at 590 nm for the low pg level detection of the anti-tumor drugs adriamycin (A_1) and daunorubicin (D_1) in human urine (31).

A sub-microliter fluorescence flowthrough cuvette suitable for monitoring HPLC effluents has been developed (32). The cuvette was constructed based on the sheath flow principle, in which the chromatographic effluent is injected into the center of an ensheathing solvent stream but does not mix with it because laminar flow conditions are maintained. A sample volume adjustable from 6 to 150 nL can be manipulated by varying the relative flow rates of sheath and effluent. Since the windows are not in contact with the sample flow, the stray light from the windows is reduced. A detection limit of 53 pg for test compound was accomplished.

Proper detector cell design can contribute significantly in the reduction of background fluorescence emission which hampers the attainment of better fluorescence detectability. A laser-based detector with the flow cell arranged in the form of a free-falling thin jet was designed for conventional HPLC column. For microcolumn effluents, a quartz capillary tube was used to avoid drop formation. The miniaturization was intended for minimizing the post-

column band broadening. The excitation source was provided by a krypton ion laser operating at 351 and 356 nm in a CW mode with a total power of 1W. The lowest detection limit was a commendable 20 fg for fluoranthene with the emission wavelength set at 450 nm. The illuminated volume of the two laser detector was about 1 nL while the dead volume was around 1 μl, about one-fifth of that of a commercial LC fluorimeter (33).

By combining the energies and polarizations of two photons in a single quantum jump between two molecular states, the simultaneous absorption of two photons by a molecule enables one to explore and exploit the spectroscopic region which is inaccessible to ordinary one-photon spectroscopy. This simultaneous absorption of two photons in a single act requires no stationary intermediate states to match the energies of the photons. Another way to reach high excited states is through sequential promotion involving two successive single photon absorptions in which a real intermediate state is required. Two-photon absorption spectroscopy observes a different set of selection rules due to symmetry considerations (34-37). It is an inherently weak process with very low transition probabilities. However, significant enhancement in absorption strength can be obtained by the large photon fluxes of lasers (34).

The subsequent fluorescence after two-photon excitation can be monitored using highly efficient photon counting techniques. The added dimension for spectral selectivity more than compensates for its more restrictive applications since less compounds will be able to participate in this process.

The sensitivity and especially the selectivity of a laser two-photon excited fluorescence HPLC detector (35) was demonstrated for the separation of the oxadizaoles PPD, PBD, and BBD in the presence of several polyaromatic hydrocarbons (PAH). Two photons of 514.5 nm radiation from the same argon ion laser with a power rated at 4 watts were focused to a very small spot in a simple capillary flow cell. Since the excitation is in the visible and the fluorescence is in the UV region, a very low detection background was achieved due to the elimination of Rayleigh and Raman scattering. The spectral separation of background signal coupled with the high power density of excitation made possible nanogram detectability, which is comparable with UV absorbance detection of compounds with moderate two-photon absorption strengths.

Asphaltene fractions of solvent-refined coals are known for their complexity due to abundance of medium molecular weight, unsaturated organic compounds. The simplification of chromatogram and information extraction can be better served by putting selective detectors in series. By

arranging the different detectors in three dimensions, thanks to the fiber-optics based flow cell design (31), simultaneous chromatograms from a commercial UV absorbance detector (fixed wavelength at 254 nm), a laser excited one-photon (488 nm) visible fluorescence detector, and a two-photon laser (488 nm) excited UV fluorescence detector can be obtained. The chromatograms were found to be good fingerprints for the classification of individual solvent-refined coals (36).

In the two-photon absorption process, if there is an in-intermediary state which can resonantly enhance the absorption, selectivity can be gained over species without the intermediary state (22, 34). The above principle was applied in constructing a sequentially excited fluorescence HPLC detector (38), wherein fluorescence is monitored from a highly excited molecular state following sequential resonant excitation using a tunable laser source.

Another scheme of HPLC detection is based on laser-induced absorption. If a laser is used as the light source, large amounts of heat can be generated along the optical path inside the liquid due to the sample absorption of the high laser photon fluxes. If the laser is modulated, periodic production and dissipation of heat will generate acoustic waves in resonance with the modulation frequency. This photoacoustic effect can be detected if proper

transducer and phase-sensitive devices are employed. Oda and Sawada (39) constructed a flow cell in which a piezoelectric transducer (PZT) disk was made to contact the liquid through a very thin (0.1 mm thickness) polished platinum foil. With the modulation frequency set at the optimum value of 4 kHz for lock-in detection, the LC separation of three chloro-4-(dimethylamino)azobenzene isomers were monitored by this laser-induced photoacoustic detector. Although the test compounds have limited molar absorption coefficients at the 488 nm of laser excitation, a 7.0×10^{-6} in absorptivity was obtained. This value represents a 25-fold improvement in sensitivity over UV detection.

Thermal lens calorimetry is another means of probing the absorption process through the use of laser heating. The Gaussian intensity distribution of a laser beam causes an uneven absorption among molecules residing in the interaction zone created by the propagation of the laser through the medium. The release of absorbed energy in the form of heat results in a temperature gradient and induced refractive index gradient in the confined region. The decrease in refractive index due to the temperature increase is equivalent to the formation of a diverging lens in the optical path and the term thermal lens adequately summarizes the whole effect (40, 41). The light collected behind a pinhole is controlled by the degree of beam divergence. A

chopped laser beam would be able to create a time-dependent light intensity variation if an absorbing species is present within the beam profile.

The above thermal lens calorimetry was applied to the chromatographic detection of nitroaniline isomers (42), which have negligible fluorescence quantum yields. Using the 458 nm line of an argon iron laser at a 190 mW power level, one can detect 1.5×10^{-5} in absorbance with a 5 second response time.

Infrared spectroscopy (IR), due to its recognized fingerprinting capability on molecular species, can also be applied to LC detection. In this method an IR detector is set at one of the wavenumber ranges that is a characteristic absorption of some functional group and the absorption is then measured. In a LC system (43), the 3.39 μm line of a helium-neon laser with 1 mW power was used as the infrared laser source. In wavenumbers this wavelength corresponds to 2950 cm^{-1}, and it falls within the region of a C-H stretching vibration. It is expected that a majority of organic compounds will absorb this radiation and be detected. The minimum detectable amount was determined in the low microgram range for samples like tripalmitin and cholesteryl palmitate.

However, this procedure precludes the use of many

hydrocarbon solvents in favor of halocarbons like CCl_4, $CHCl_3$, and C_2HCl_3. In this method, besides the limitation on the choice of solvents and columns, it is impossible to set at any wavenumber range if the nature of the sample is not known in advance. The limited tunability and power of some of the existing infrared sources is also problematic.

The argon ion laser is the most familiar light source of the commercial laser Raman spectrometer. Coupling a Raman spectrometer with HPLC requires no interface since the small flow-through cell can be placed at the exit of a LC column and serve as the detector cell. However, for LC detection, the Raman emission from the components in the LC effluent are easily overwhelmed by the accompanying, more abundant solvent scatters and this results in its limited application. One remedy is to exploit the improvement of Raman scattering efficiency offered by resonance-enhanced Raman spectroscopy (44) where the excitation laser wavelength is set near, or at an excited electronic state of the molecule of interest. This approach was adapted for the on-line detection of mesogenic azoxybenzenes by a combined HPLC/Raman spectrometry technique (45). The excitation wavelength was set at 458 nm to meet the resonance requirement. By electronically subtracting the interfering contribution from pure eluting solvent, a detectability of the order of 1 μg was reported. The presence of fluorescence can obscure the Raman signal

even under the resonance enhancement condition, a new Raman technique can be brought in to alleviate this problem. CARS (coherent anti-Stokes Raman spectroscopy) is a unique nonlinear optical process made possible by high power lasers. Light waves of different input frequencies, w_1 and w_2, are mixed together in a material medium (liquid, solid, or gas) to generate a new frequency, w_3, which appears in a coherent laser-like beam. When w_3 corresponds to a Raman-active molecular vibration or rotation (or electronic transition), then the CARS effect is strong and easily detected (46).

The near total rejection of fluorescence in CARS can be attributed to: (a) the CARS emission at w_3 occurs at a higher frequency than either of the excitation frequencies (whereas, fluorescence occurs at lower frequency), and b) the energetic laser-like beam of CARS radiation may be completely collected as compared to the very small fractional collection of nondirectional fluorescence over 4π steradians (solid angle). Carreira et al. (47), and Rogers et al. (48) developed a computer-controlled LC/CARS detection system. Two nitrogen-pumped tunable dye lasers (260-740 nm) were used for the excitation process. When monitored at 430 nm, a detection limit of 1 μg has been calculated for β- carotene.

The most recent entry in the laser-based detector development has been the use of Fabry-Perot interferometry and a stable He-Ne laser for the sensitive detection of refractive index changes. The finesse of an interferometer determines its ultimate resolution which is reflected in the sharpness of the interference peaks. The sharper the peaks, the easier it is to locate their positions precisely. The added finesse provided by a high quality plane parallel Fabry-Perot interferometer will lead to increased sensitivity in measuring changes in refractive index. To function as an RI detector for LC, the interferometer, with the flow cell placed inside its cavity, is scanned by applying a computer-controlled voltage ramp across the piezoelectric crystal. During each ramp cycle, the output of the photomultiplier tube (PMT) is digitized and stored in the computer at fixed time intervals. The maximum PMT output in each scan is converted to an analog signal, which is proportional to the RI, for recorder display. The achieved detectability is 1.5×10^{-8} and 4.0×10^{-9} RI units for benzene in acetonitrile for single beam and double beam operation, respectively (49). This is roughly one and two orders of magnitude, respectively, improvement over those of commercial RI HPLC detectors. If a second more powerful laser is used to interact with the analyte, absorption can be indirectly monitored as a change

in refractive index. Detectability of 2 orders of magnitude better than a standard HPLC absorption detector was achieved (49).

Besides the above-mentioned laser-based detectors, a completely different mode of detection, based on nephelometry, was also developed (50). After the post-column addition of a precipitating agent to generate the turbid components for scattering, a low power He-Ne laser was allowed to interact with the precipitates and the scattered light was used for the microgram level detection of nonpolar lipids. It is also of interest to note that a windowless flow cell capable of fitting into a sensitive detector for LC application may be constructed which employs fluorescence, photoacoustic, and photoionization (one or two-photon) modes of operation (51) that would advantageously complement each other's function.

Conclusion

So far, we have seen a variety of ingenious laser techniques that are being developed for liquid chromatographic detection. These methods involve a wide range of sophistication but all exploit the spectral advantages of the coherence or high power of lasers. The interest in laser-based HPLC detectors is increasing rapidly as

illustrated by the work of many laboratories throughout the world. Taken together, it is clear that the trend will continue in the future, especially with the extension of laser sources to cover even greater ranges of wavelengths.

CHAPTER III. LASER OPTICAL ACTIVITY DETECTION FOR HIGH PERFORMANCE LIQUID CHROMATOGRAPHY

Introduction

The first discovery of the phenomenon now known as optical activity, was made by the French physicist Dominique Arago in 1811. He found that the plane of vibration of a beam of linearly polarized light underwent a continuous rotation as it propagated along the optical axis of a quartz plate (52). In 1818, Jean Baptiste Biot, another French physicist, saw the same effect while working with several naturally occurring organic compounds such as sugar, tartaric acid, turpentine, and camphor, whether they are in the liquid state, in the vapor state, or dissolved in solution (53). This field took on a new importance in 1818 after Louis Pasteur's pioneer work of resolving two isomeric configurations of optically active sodium ammonium tartrate crystals with only a hand lens and tweezer (54). Not until 1874, however, did Jacobus van't Hoff and Joseph Le Bel independently recognize that every optically active organic compound known at that time possessed at least one asymmetric carbon atom, which was defined to be a carbon atom surrounded by four different univalent groups (55). Although van't Hoff's attempts to rewrite planar chemical formulas in three dimensions to support his hypothesis were

coolly received initially (56), this tetrahedral geometry eventually proved to be correct and played a fundamental role in the development of the ideas of modern stereochemistry. Since then optical activity is considered a very useful tool in structural chemistry because of its sensitivity to the arrangement of the atoms in the molecule.

Conventionally, a substance which, in the absence of external influences, rotates the plane of linearly polarized light is said to be optically active or to possess optical rotatory power. The necessary condition for exhibiting optical activity is the nonsuperposability of molecule and its mirror-image, dissymmetry, as suggested correctly about 130 years ago by Pasteur. This requires the absence in the molecule of the following: a plane of symmetry ($\sigma = S_1$); a center of symmetry ($i = S_2$); an improper axis of rotation in the strict sense (S_n) (55).

While the structural requirements for optical activity can be precisely defined, the mechanism in which the plane polarized light interacts with a material substance to cause rotation is much less obvious than the processes responsible for absorption, emission, or refraction (73). Optical activity can be related by refractivity or scattering theory to the interactions of electric and magnetic multipoles induced in each molecule by the electric and magnetic

fields of the light wave (57). The rigorous treatments of the theories of optical activity, as expounded by Rosenfeld (58), Kirkwood (59) and others (60), generally involve the use of molecular wave functions, quantum-mechanical analyses of transition and perturbation, stereochemical symmetry rules and some higher level mathematics like tensor. The lengthy equations are helpful but do not provide much physical insight for the clear understanding of the relationship between molecular structure and optical activity. For those who are interested in further exploring the theoretical aspects of optical activity, the review article by Mason (61) and a book by Caldwell and Eyring (62) are also recommended.

The much simpler phenomenological explanation of optical activity was proposed by Fresnel back in 1825 (52), without addressing himself to the actual mechanism involved. He assumed and experimentally proved that linearly polarized light can be represented as a superposition of two opposite circularly polarized light components. An optically active material has one index of refraction, n_R, for right circularly polarized light, and another, n_L, for left circularly polarized light. The possession of two indices of refraction for circular polarized light is called circular birefringence, or circular double refraction (63). Since an index of

refraction is deemed as $n_i \equiv \frac{c}{V_i}$, where c is the speed of light in a vacuum and V_i is its speed in the medium, Fresnel's hypothesis means that there is a difference in speed within an optically active medium for the two types of circularly polarized light. In traveling through an optically active medium the two circularly polarized components would get out of phase and the resultant linearly polarized light would appear to have rotated. The amount of rotation of the plane of polarization, α, is given by (52).

$$\alpha = \frac{\pi d}{\lambda_0} (n_L - n_R) \qquad (1)$$

where d is the thickness of the medium and λ_0 is the wavelength of the light, in vacuo. It can be seen that one must distinguish between right- and left-handed rotation. If, while looking in the direction of the light source, the plane of polarization appears to have revolved clockwise, the rotation is designated positive, the substance is referred to as dextrorotatory or d-rotatory. Alternately, if the plane appears to have been displaced counterclockwise, a negative rotation is assigned, and the material is said to be levorotatory or l-rotatory (52). It is noted from the above equation that a substance with $n_L > n_R$ is d-rotatory and is l-rotatory if $n_R > n_L$. The difference in refractive indices for circularly birefringent materials generally is

of the order of 10^{-4} to 10^{-8} (64). For example, in sodium light the specific rotatory power, which is defined as α/d is found to be 21.7°/mm for quartz. Thus, it follows that $|n_L - n_R| = 7.1 \times 10^{-5}$ for light propagating along the optic axis (52). The rotatory power of liquids in comparison is so relatively small that it is usually specified in terms of 10 cm path lengths; for example, in the case of a solution of 3.45 g of sucrose in 100 g of aqueous solution, the circular birefringence is only 2.77×10^{-6} at 18°C with $\lambda = 500.0$ nm (64). From the above equation, it is readily shown that the experimental variables that influence the extent of rotation include the thickness of the layer in the path of the radiation, the wavelength of the radiation used for the measurement, and the temperature.

In the case of solutions, the concentration of optically active material is also involved, and the nature of the solvent may also be important. To incorporate such effects into the record under a set of standard conditions, the observed value of rotation, α, is converted into a ratio, $[\alpha]$, the specific rotation, expressing the number of degrees per unit concentration per unit of path length (65). By definition

$$[\alpha]_{\lambda}^{t} = \frac{100\ \alpha}{c\ell} \qquad (2)$$

where

c = concentration in grams of solute per 100 ml of solution

ℓ = length of the light path in the solution, measured in decimeters (1 decimeter = 10 cm)

α = observed rotation in degrees (plus or minus)

λ = wavelength of light used (generally at 589 nm, the D line of a sodium-vapor lamp)

t = temperature of the solution in degrees centigrade (the standard temperature is 20°C)

The specific rotation of a compound is an important physical constant, comparable to its molecular weight, density, refractive index, melting point, boiling point, etc. It is one more physical characteristic that a chemist can use to identify a substance or determine its optical purity. Moreover, by measuring the actual rotation α of a substance of known specific rotation $[\alpha]$ in a sample tube of fixed length ℓ, one can readily calculate the concentration c of the solution. This quantitation application is perhaps the most useful to the analytical chemist.

The instrument used to measure the number of degrees of rotation of plane-polarized light by optically active compounds is called a polarimeter. The principal components of a basic polarimeter include a monochromatic light source, a polarizer to produce plane-polarized light, a sample tube of cylindrical design for holding solutions in the light

path, an analyzer (actually, just another polarizer) to set the crossed position that yields a minimum transmission of light in the absence of an optically active sample, and a scale in a detecting system to measure the amount of rotation. Some of the major manufacturers of commercial instruments designed to measure optical rotation at one or several wavelengths (ORD) are O. C. Rudolph and Sons, Bendix, Carl Zeiss, the Perkin-Elmer Corp., Japan Spectroscopic Co. (JASCO), and the Cary Instrument Co.

The details of various types of experimental techniques and physical optics of polarimetric measurements are dealt with in great length by Heller and Curme (66). Polarimetry, besides being a well-recognized method in elucidating the structure of optically active compounds, could also be a logical and legitimate mode of detection for HPLC, in view of the ability of automatic polarimeters to provide extremely accurate rotation measurements rapidly. However, the adaption of a commercial spectropolarimeter for use as a HPLC detector has been restricted due to instrumental limitations, technical difficulties, as well as the accessibility of this instrument. In the first place, the interaction volume of several mL in the sample cell is not small enough to preserve a reasonable resolution after the separation. Secondly, the lack of

sensitivity makes it unattractive to most chromatographic applications, especially in the biomedical fields. The sensitivity of polarimeter detector for HPLC was discussed from a theoretical point of view (67), and a detectability of a minimum concentration of $C_{min} = 3x10^{-4}$ g/cm^3 was established under the most favorable conditions (such as $\alpha_{min} = 0.0015°$). Although practically achieved sensitivity was not presented in this case, an order of magnitude degradation should be a reasonable estimate, based on the performance of a Bendix-NPL automatic polarimeter which was equipped with a modified micro-cell of 110-µl volume for use with an ion exchange column (68). In this work, a sensitivity corresponding to a full-scale deflection of 0.01° degree rotation resulted in a noise level of 25% of the full-scale deflection. Alternately, the optical activity as circular dichroism (CD) (differential absorbance for left- and right-circularly polarized light, $\Delta A = A_L - A_R$) of the eluent from an LC column was monitored by a modified spectropolarimeter, operating in the CD mode (69, 70). The detection limit is in the µg level at selected wavelengths (70). Recently, Boehme and coworkers (71) directly connected a variable wavelength UV detector with a general purpose Perkin-Elmer Model 241 spectropolarimeter in series for the combined quantitation of trans-PBE enantiomers. The response from the UV detector provided the basis for the examination of the total amount of trans isomer, while the polarimetric

signal is proportional to the R and S enantiomer ratio. Even with the use of a shorter wavelength of 302 nm to take advantage of a higher specific rotation, and with the use of a newly designed micro flow cell (72) having a 10-cm optical pathlength and much smaller geometric volume of 33 µl to avoid the peak broadening, the high detection limit of 60 µg restricts its usefulness considerably due to the requirement of relatively large amounts of injected materials. These instances point to the inadequacy of trying to employ a conventional polarimeter as a legitimate optical activity detector for HPLC. In order to effectively overcome the drawback of the inherent low sensitivity in a polarimeter and extend its application capability, a new instrumental approach is warranted. In this work we have therefore completely redesigned a detector for measuring polarization rotation that is suitable for monitoring optically active components in the column effluent of HPLC.

Detector Design

In this section, we shall summarize the critical design parameters that led to the working optical activity detector and in the mean time examine some of the unique and relevant properties of a laser that is advantageously used to make the construction of this instrument possible.

Polarizer

Linearly polarized or plane-polarized light is light for which the orientation of the electric field is constant although its magnitude and sign varies in time. The electric field vector therefore resides in what is known as the plane of vibration. The locus of the tip of the electric vector is a straight line and this is why the light wave is said to be linearly polarized. The angular orientation of the straight line is also known as the direction of polarization (74).

A perfect polarizer is a device from which the emergent beam is linearly polarized, regardless of the state of polarization of the incident beam. Any component of the incident beam whose direction of polarization is at right angles to the transmission axis of the polarizer is rejected. However, a perfect polarizer is not realizable in practice, as the rejection of the component orthogonal to the polarizer axis is never complete. For the light source the output of many lasers is linearly polarized, with the ratio of the light polarized in one direction exceeding that polarized in the orthogonal direction by 1000:1 as a result of Brewster surfaces within the laser (75). The presence of Brewster windows assures that light of one polarization direction is transmitted out of the lasing medium to the

reflecting mirrors and back into the lasing medium with no loss. For light polarized perpendicular to the plane of incidence, the reflection loss at the Brewster surface makes it impossible for the light of this polarization to lase (75). This high degree of linear polarization of the laser greatly enhances the efficiency of polarizers. In polarimetry the performance of the polarimeter depends on the extent it can reject light of the improper polarization in a crossed polarizer-analyzer pair. This critical parameter here is defined as the extinction ratio, which is the amount of light transmitted in the correct linear polarization versus the amount transmitted along the extinction axis.

Laser technology relies heavily on birefringent natural calcite ($CaCO_3$) as a linear polarizer. Its availability in sufficient size with optical homogeneity outweighs its limitations in spectral range (320 nm to 2300 nm), optical damage threshold (CW: 1 Watt/cm^2, pulsed: 5 Watts/cm^2) and obtainability for most laser applications (76). Commercial polarizers of the highest quality are generally of the Glan-Thompson design and provide an extinction ratio of 10^6. The major factor in limiting the attainable extinction ratio have been shown to be directly related to the crystalline defects of the calcite in crossed high quality Glan-Thompson polarizers. The large difference in defect density and the effect of these defects on the

polarization behavior explain the orders of magnitude difference in the efficiency of Glan-Thompson polarizers manufactured under identical conditions (77). This also indicates that the extinction ratio can depend strongly on beam size and lateral placement of the prism in the beam because the smaller the beam, the more likely is the chance of using more uniform subregions of the crystal. The directional property of the laser can be advantageously used in locating the good localized regions over the long separation between polarizer and analyzer. The reason for this is that lasers are inherently sources with low divergence due to the geometric characteristic of the optical resonator of the laser cavity. One can easily show that a typical laser with beam divergence of 1 milliradian increases in size about 1 mm for every meter of beam travel. This high collimation of the light beams makes the delicate manipulation of beam optics very easy to accomplish. In this work, the argon ion laser, with its stable output, high intensity, visible radiation and small beam size, was used to provide good collimation in scanning and locating regions of good extinction in the polarizers. This directional property also offers the opportunity of using small apertures along the optical path for spatially filtering the scattered light. We have confirmed Moeller and Grieser's finding (77) that using a second tandem analyzer does not improve the extinction ratio since

it is necessarily oriented in the pass direction of the first analyzer. Within the calcite crystals with imperfections (scattering centers and strain), the half of the polarizer away from the source and the half of the analyzer toward the source are the major contributing parts. It was also observed that not only did the measured extinction ratios vary from prism-to-prism but also were different when the prisms were turned end-to-end. Taking those observations into account, we found that by selecting specific combinations of crystals as analyzers and polarizers, and specific combinations of entrance and exit faces for each, an extinction ratio of 10^{10} could be obtained in one of the many combinations for four Glan-Thompson prisms. The worst case among those combinations, however, still meets the manufacturer's specification of 10^{6}. The extinction ratios were determined by measuring the laser power and by estimating the number of photons actually transmitted from a knowledge of filter transmittance, natural reflection off each surface, phototube quantum efficiency, and measured photon count rate. In one experimental set-up, a monochromator was placed behind the polarizers but in front of a photomultiplier tube which was connected to a photon counting system. When the polarizer and analyzer were parallel, the power of the 514.5 nm line of argon ion laser as measured behind the analyzer was

0.25 watts, which is equivalent to a photon flux of 6.5×10^{17} photons per second. With polarizer and analyzer crossed, the photon counter registered 1.5×10^{6} counts per second. Including a factor of 0.15 for the quantum efficiency of the photomultiplier tube and a factor of 0.5 for the transmission efficiency of the monochromator, the number of photons transmitted under parallel condition with that under crossed condition, the extinction ratio was calculated to be 3.25×10^{10}. An important observation is that the 10^{10} extinction ratio can be routinely achieved after the initial trial-and-error process, even after one full year of use. It is interesting to note that an extinction ratio of 10^{10} is equivalent to having "noise" from 5.7×10^{-4} degree misalignment using perfect polarizers and analyzers. For this reason, the prisms must be rigidly mounted and must have fine angular adjustments. Our original mounting plates of aluminum show enough deformation when torque is exerted by hand to one end that one actually can detect a poorer extinction ratio (78).

Flow cell

In general, all present-day LC detectors are on-stream systems, continuously monitoring certain characteristics (refractive index, UV absorption at a given wavelength, etc.) of the column effluent in a flowthrough cell. The excellent

collimation property of the laser implies that small detector volumes can be achieved to avoid mixing after separation. However, the detectability in polarimetry can be proportionally enhanced by using long pathlength cell. So, the design of a flow cell must be a compromise between having a long interaction path and a small cell volume to preserve chromatographic resolution. To maintain a relatively uniform beam radius over distance in a focused Gaussian beam such as the laser, we have

$$Z = \pi\omega^2/\lambda$$

where Z is the Rayleigh range, the range of collimation of the focused beam, λ is the laser wavelength selected, ω is the beam radius at the $1/e^2$ intensity point, and all three have the same length units. For a pathlength of 10 cm and using 500 nm light (actually both 488 nm and 514.5 nm lines of argon ion laser are used in the work), we can calculate that the beam radius at the waist is 126 μm. Since 2ω gives the 1/99 intensity point and the beam size at the extremes of the Rayleigh range is twice that at the waist, the radius of the cell bore should be 500 μm, corresponding to a cell volume of 80 μL. In the actual construction of the cell, we are limited by the available size of a drill bit for such a long bore. In the end, a 1/16" diameter hole of 10 cm (4") length was drilled to be the interaction region

which in turn corresponds to a 200 μL cell volume. It was pointed out that a flow cell volume of up to 25% of peak volume would not cause significant loss of chromatographic resolution (79). Although improvement can still be made in this respect, the 200 μL cell volume here should contribute little to the broadening of the chromatographic peaks since each typically has a peak volume of 1 mL under normal experimental conditions. Naturally, depending on whether one is interested in trace analysis or microanalysis, the optimum dimension of the cell will change.

In a polarizer-analyzer combination, complete extinction cannot be re-established if the state of polarization is transformed from linear polarization into elliptical polarization by the addition of other optical elements in-between (66). One possible source of ellipticity are lenses and window materials that are rarely free of stress birefringence. It is imperative to avoid the use of lenses or prisms between polarizer and analyzer. It is further desirable that the additional scattering centers and birefringence introduced by the indispensable windows on the flow cell be reduced to a minimum. Various window materials including the highest quality laser optical windows and optical flats were tested using our selected polarizer-analyzer combination. We learned that the use of a thin

window material with a reduced optical path, though less rigid, did provide a better solution.

Standard commercial cover slips were chosen for cell windows, and we found that about 1 in 10 or less, depending on personal skill and patience, showed considerable areas (a few mm^2) of good enough optical quality that the 10^{10} extinction ratio was maintained with these in place. The procedure for selecting a desirable cover slips as cell window is described below. First, the flow cell should be properly aligned to establish an unobstructed light path through its center bore and maintain the original extinction point. The dc current output, read from a digital multimeter, from the photomultiplier tube is used as the extinction indicator during the whole process. For a 20-mW 514.5-nm argon ion line measured at the flow cell, a current value of around 2 μA is typical when the 56 DVP photomultiplier tube operated at 1700 V is used. A cover slip is then held directly against the polished surface of the flow cell. To locate the good optical region within the cover slip, one can laterally and rotationally move the cover slip around the entrance or exit end of the center bore. The orientation of this cover slip relative to the center hole is carefully marked as soon as the current value is again near or at the previous reading. In fact, in certain cases, the resulting

extinction ratio was improved, probably due to partial cancellation of the birefringence in the polarizing prism. Mounting these cover slips present additional problems since they must remain strain free. We ruled out an O-ring seal approach and decided on a silicone cement which remained slightly flexible even when cured. The removal of old windows is also made easier since only the use of razor blades is required. We were concerned that pulsation during the pump cycle of the liquid chromatograph might distort the windows to introduce strain-induced birefringence. This was later not found to be a serious contribution to noise. Once the windows were in place, little deterioration occurred over long periods of time.

Faraday rotators

The simplest method of measuring a rotation caused by the presence of an optically active sample would be by determining the angle through which the analyzer must be rotated in order to re-establish complete extinction (i.e., minimum transmission of light after the analyzer). However, the identification of a reference point at minimum transmission as required by this method cannot be done with precision either by the eye or a phototube (80). The precision can be significantly improved by the use of half-shade principle which establishes the reference point

at an analyzer setting a few degrees away from the extinction point to have a reasonable level of light intensity (73). However, it is certainly not practical to apply these techniques under the gradually varied rotation situation as would be expected in a chromatographic system.

The modulated null-balance method presents a very convenient approach for single beam polarimetric operation. Here the plane of polarization of the beam incident upon the analyzer is made to oscillate through a small angular range, which when the instrument is near balance, includes the extinction angle. This normally can be done in one of two ways: mechanical null-balance or electrical Faraday effect null-balance. In mechanical null-balance, the modulation is brought about by oscillating the polarizer or the analyzer with the help of a servomotor. However, one can not hope to produce mechanical rotation to an accuracy and angular stability much below 10^{-3} degrees. We, therefore, used a system similar to that of the Bendix recording spectropolarimeter which employs an ac-modulated Faraday cell to obtain a null-balance electrically.

Michael Faraday, in 1845, found that when plane-polarized light passes through a light-transmitting medium in a direction parallel to the lines of force of an externally applied magnetic field, the polarization plane of the

light wave is rotated. The angle (measured in minutes of arc) through which the plane of polarization rotates in given by the empirically determined expression (52)

$$\alpha = V \cdot B \cdot L \qquad (3)$$

Here, V denotes the magneto-optical rotation constant or Verdet constant (in min. of arc gauss^{-1} cm^{-1}) and is dependent on the nature of the medium, the temperature, and the wavelength of the incident light. B is the magnetic field strength (in gauss) and L is the length of medium traversed (in cm). In optics, the Faraday effect has been utilized to build a polarization modulator in the form of a solenoid. When the medium and length are fixed, the Faraday rotation is controlled by the strength of the magnetic field which in turn is regulated by the coil current. By way of Malus's law, the polarization modulation is converted to amplitude modulation by the analyzer whose position is fixed relative to the polarizer and the amplitude variation of the emerging light beam is then a function of the modulation voltage across the coil.

A brief description of the modulation scheme coupled with phase-sensitive detection (lock-in amplifier) is in order. In Figure 1, the axes are chosen as the laboratory frame of the analyzer, i.e., light linearly polarized in the

x-direction is totally transmitted while light in the y-direction is rejected, to the extent of the extinction ratio. For a modulation angle of α, the maximum amount of light transmitted can be found as the projection of the electric field vector on the x-axis, or E sin α, where E is the field amplitude. The intensity, being proportional to the time-average square of the electric field then has a sine squared dependence (the law of Malus) and we have

$$I_{trans} = I_o \, Sin^2\alpha \qquad (4)$$

where I_o is the maximum intensity, transmitted when $\alpha=90°$.

The optimum modulation is from an angle α to an angle $-\alpha$ from the y-axis, so that the lock-in signal is zero. When an optically active sample is present, the modulation is then from $\alpha+\delta$ to $-\alpha+\delta$ with δ being the angle of rotation introduced by the sample. The lock-in signal is then proportional to:

$$I = I_o[\sin^2(\alpha+\delta) - \sin(\alpha-\delta)] \qquad (5)$$

where I is the transmitted intensity.

The above equation can be simplified to:

$$I = I_o \sin 2\alpha \cdot \sin 2\delta$$

after applying the trigonometric identities involving powers

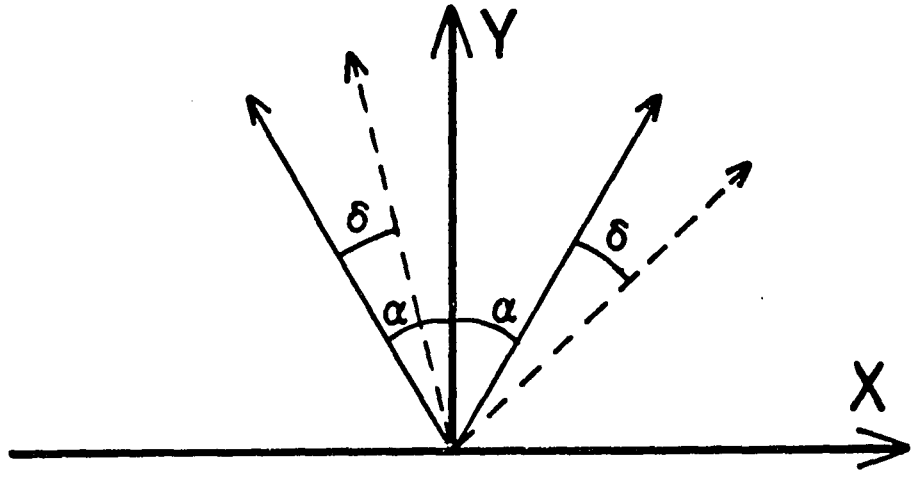

Figure 1. Vector diagram for polarization modulation

and sums.

In the range of interest, α and $\delta < 10^{-3}$ degrees. For such a small angle, the sines can be replaced by the angle values, and we have

$$I = 4I_o \alpha \delta \qquad (6)$$

It is therefore desirable to use as large a modulation as possible, provided that the stability of the modulation is better than δ. It is further noted that during the absence of either optically active material or angle modulation, the lock-in output is equal to zero. The modulation frequency is arbitrary, and was chosen in this work to have a current waveform in the Faraday rotators close to a square wave and also to coincide with a relatively noise-free region in the laboratory environment.

Normally, Faraday rotators in polarimeters employ quartz, glass or a liquid such as water to take advantage of their much larger Verdet constant (see Appendix A). The chosen medium in the form of a cylindrical rod was surrounded by a coil wound with copper wire. In order not to introduce any additional scattering centers or strain-induced birefringence caused by the medium itself or the windows needed to contain the liquid, we decided to base our Faraday rotators on air (Verdet constant is 6.27×10^{-6} min of arc gauss^{-1} cm^{-1} at $\lambda = 578$ nm, p = 760 mmHg and

T = 0°C) as the medium. Two modulating and one compensating Faraday rotators are used in this work. The modulating Faraday rotators were constructed by winding 16,750 turns of 26 a.w.g. heavy armored polythermalenze magnetic wire (total resistance 160Ω) along with 20 cm long, 4.6-mm i.d., thick-wall nonferromagnetic 316 stainless steel tubing. The compensating rotator is of similar design with 8000 turns of 30 a.w.g. magnetic wire (total resistance 100Ω) wound along a 10 cm long, 4.8 mm o.d., thin wall stainless steel tubing. A rough calculation shows that both kinds of solenoids produce a field of 1000 gauss per ampere of current applied. This translates to 1 and 2 millidegrees of rotation per ampere for compensating and modulating Faraday rotators, respectively. This is an unusually small amount of modulation, but can be shown to be adequate for our applications (see Appendix A for more detailed discussion on the Faraday rotators).

Experimental

A schematic of the experimental set-up of the laser-based HPLC optical activity detector is shown in Figure 2. A Control Laser (Orlando, Fla.), Model 554 argon ion laser, operating in the 514.5-nm single line mode was used in this study. The laser output at the flow cell was made

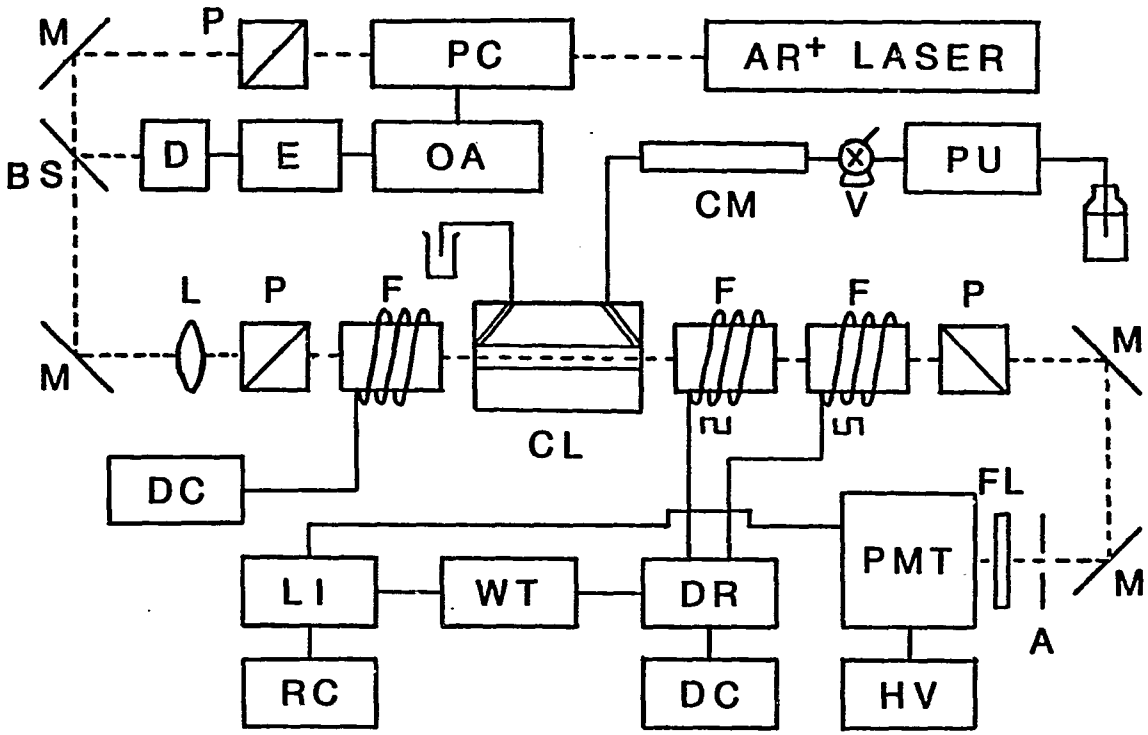

Figure 2. Experimental arrangement for the laser-based optical activity detector (PC, Pockels cell; D, photodiode; E, error signal generator; OA, high voltage operation amplifier; BS, beam splitter; HV, high voltage power supply; M, Mirrors; P, Glan-Thompson prisms; F, Faraday rotator; CL, flow cell; A, aperture; FL, filter; PMT, photomultiplier tube; DR, driver; DC, power supply; WT, wave generator; LI, lock-in amplifier; RC, recorder; PU, pump; V, injection valve; CM, column; L, collimation lens)

adjustable to tens of milliwatts by placing a Glan-laser double escape window perpendicular to the laser beam. Various portions of light will be rejected depending on the magnitude of the polarization mismatch between the laser and the orientation of this prism. A 100-mm focal length crown glass lens was used to collimate the light along the longitudinal axis of the flow cell. The lens is positioned such that its focal point will lie at the approximate center of the flow cell.

A pair of selected (see above) 8-mm aperture Glan prisms, Karl Lambrecht Corp. (Chicago, Ill.), Model MGT-25E8-45, served as the polarizer and analyzer, respectively. The prisms were mounted in rotational stages with a resolution of 10^{-3} degrees, obtained from Aerotech, Inc. (Pittsburgh, Pa.), Model STS-30/R. The separation between the prisms was kept at about 1 meter to reduce stray light. Appropriate apertures were also used at various points in the optical path for the same reason. The flow cell was machined from a cylindrical aluminum rod of 10 cm (4") long and 5 cm (2") in diameter. A 1.58-mm (1/16") diameter hole was drilled along its axis as the active region, which was intercepted at both ends at 60° by 0.89-mm (0.035") bores to interface with the chromatographic connection (see Figure 3, bottom drawing). The cell was

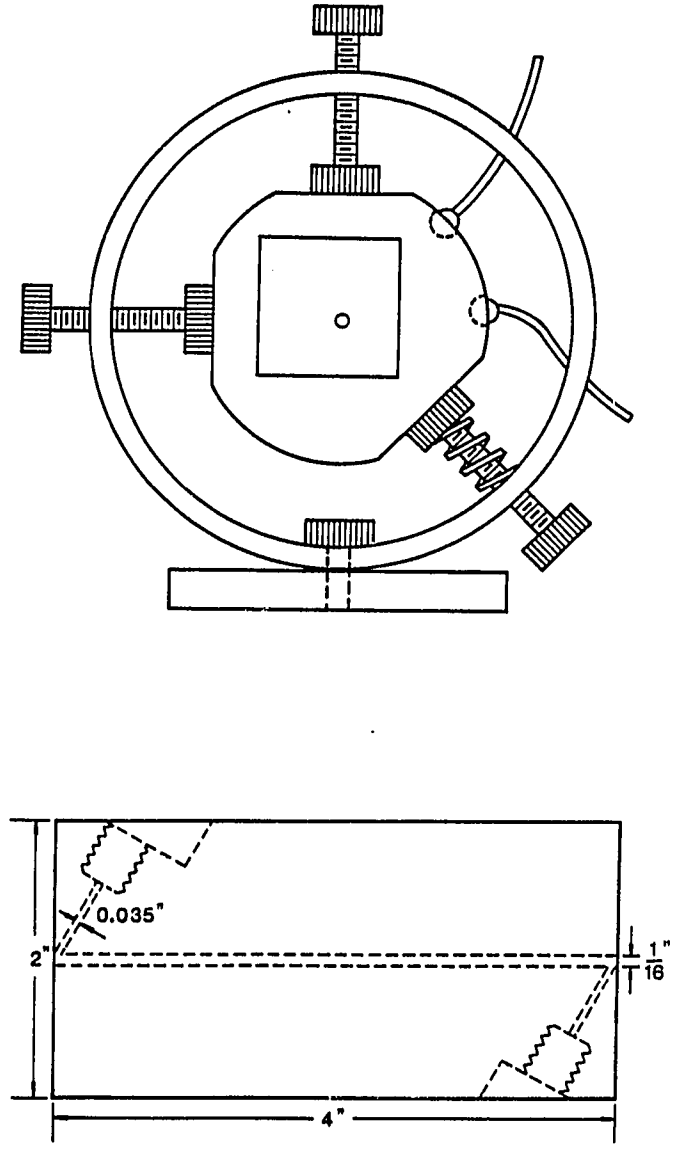

Figure 3. Spring-loaded positioner (top: cross-section of spring-loaded positioner with flow cell placed inside - bottom: side view of flow cell)

held rigidly with spring-loaded positioners at each end for optical alignment (see Figure 3, top drawing). Cell windows were selected (see above), microscope cover slips, Corning (Corning, N.Y.), Cover Glass No. 1, 25-mm square, held onto the cell by a rubber cement, Dow Corning (Midland, Mich.), Silicone Rubber Sealant. Two modulating and one compensating Faraday rotators described above were placed in the optical path. Each Faraday rotator was mounted at both ends with positioners for alignment purposes. Light is detected by an Amperex (North American Philips, Hicksville, N.Y.), 56 DVP photomultiplier tube placed 1 meter behind the analyzer. A narrow-band filter (with 30% transmission and bandwidth of 1.0 $\pm$ 0.2 nm centering around 514.5 nm) obtained from Corion Corp. (Hollistor, Mass.), Model 10-5145-1, was placed between a suitable aperture and photomultiplier tube to block the stray light. The entire assembly was mounted on a 4' x 8' x 2 1/4' optical breadboard, Newport Research Corp. (Fountain Valley, Calif.), Model LS-48, on top of a conventional laboratory bench since sophisticated vibration isolation was found unnecessary. The operating voltage of this photomultiplier tube was set at -1700V which was supplied by a Keithley Instruments (Cleveland, Ohio), Model 242, Regulated High Voltage Supply. The current output of the photomultiplier tube was terminated in a 100-KΩ resistor, and the voltage was monitored by a Princeton Applied Research

(Princeton, N.J.), Model HR-8, lock-in amplifier. The output of the lock-in amplifier was displayed on a Houston Instruments (Austin, Texas), Model 5000 chart recorder. Alternately, a Keithley Instruments (Cleveland, Ohio), Model 160B, Digital Multimeter was connected to the photomultiplier tube to monitor the current value (normally in the μA range) for best extinction. Modulation was derived from a switching amplifier circuit (Figure 4) driven by a Wavetek (San Diego, Calif.), Model 162, wave generator. DC power supply capable of delivering high current (0-1.5 A) and moderate voltage (0-200 V) was provided by Lambda Electronics (College Point, N.Y.), Model C-1580M, Regulated Power Supply. Typically, a 50-150 V, 210-Hz square wave was applied to the two modulating Faraday rotators. They are arranged in such a way that each rotator alternately modulates the light beam on either side of the extinction point in one cycle. The compensating Faraday rotator was driven by a variable, 0-50 V DC power supply for fine alignment and to provide a calibration. The laser power meter was a Keithley Instruments, Model 155, Microvoltmeter equipped with a Coherent (Palo Alto, Calif.), Model 210, thermal sensor.

Chromatography was performed in a standard arrangement using a 100-μL injection loop, a Rheodyne (Berkeley, Calif.),

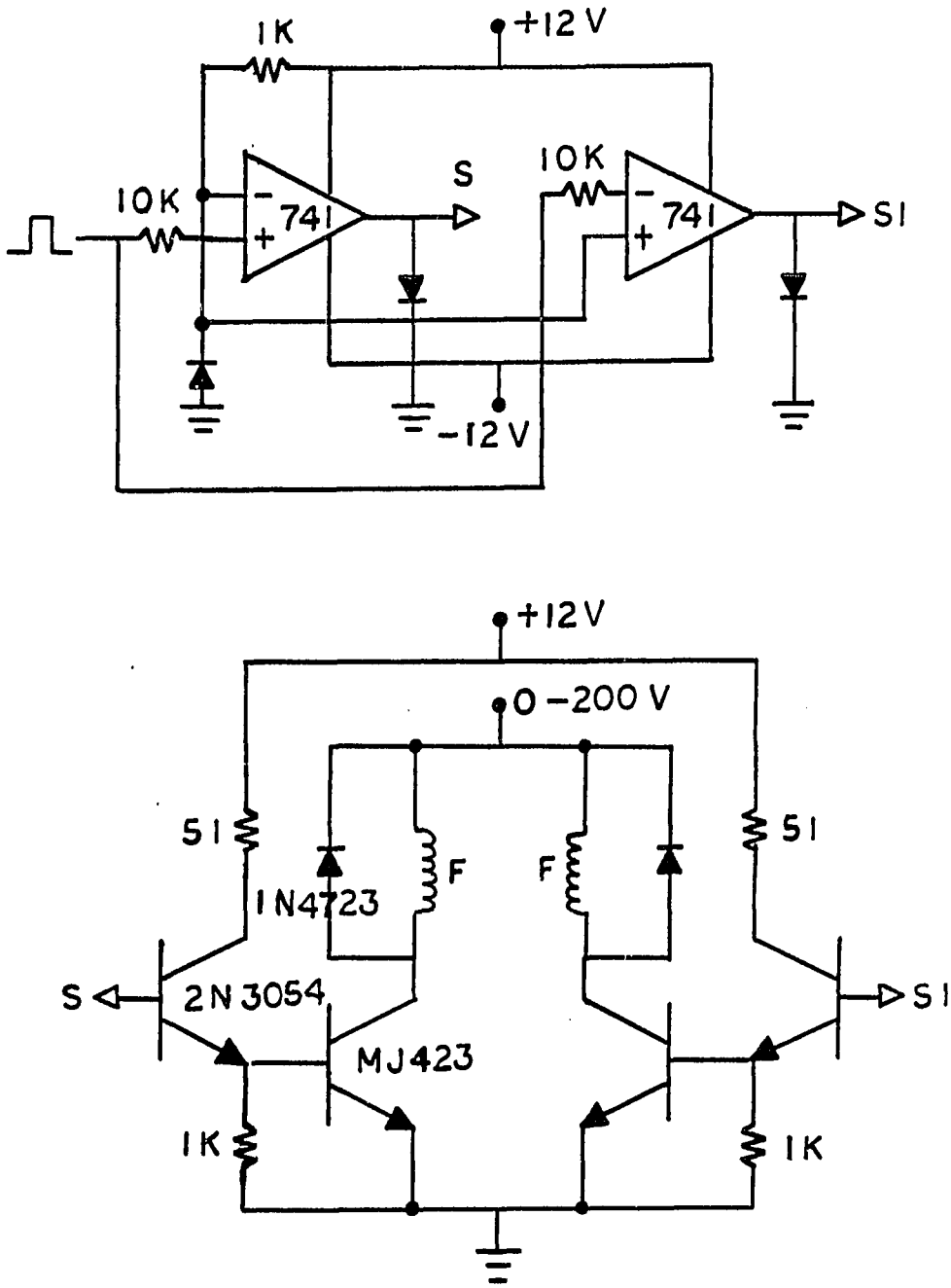

Figure 4. Switching amplifier circuit for the Faraday rotators

Model 7010, injection value, a Milton Roy (Riviera Beach, Fla.), Model 196-0066-001, minipump operated at about 1.0 mL/min and pressure fluctuations caused by the pump were reduced by using a commercial pulse dampener from Handy and Harman (Norristown, Pa.), Model Li-Chroma-Damp II. The column used was a 10-μm C_{18} reversed-phase column 25 cm long and 4.6-mm i.d. from Alltech (Deerfield, Ill.). Test sugar solutions were reagent grade materials from Fisher Scientific (Fair Lawn, N.J.), dissolved in deionized water. Deionized water was used as the eluent in this work.

Results and Discussion

To evaluate the performance of this system, reagent grade sugars: glucose ($[\alpha]_D^{20}$ = +52.7°), frustose ($[\alpha]_D^{20}$ = -92°), raffinose ($[\alpha]_D^{20}$ = +105.2°), and sucrose ($[\alpha]_D^{20}$ = +66.4°) were dissolved in deionized water to prepare the test samples. Although a C_{18} column is not the conventional choice for separation of sugars in LC, it is still possible to effectively separate glucose or fructose (both monosaccharides) from raffinose (a trisaccharide) based on molecular size difference if water, the weakest mobile phase for reversed-phase LC, is used as the eluent. Figure 5a shows a chromatogram of the separation of glucose and raffinose with 10 μg of each injected. Figure 5b shows the chromatogram of the separation of 5 μg each of fructose

Figure 5. Separation of sugars using the optical activity detector ((a) glucose (G) and raffinose (R), with 10 µg of each injected, (b) fructose (F) and raffinose (R), with 5 µg of each injected)

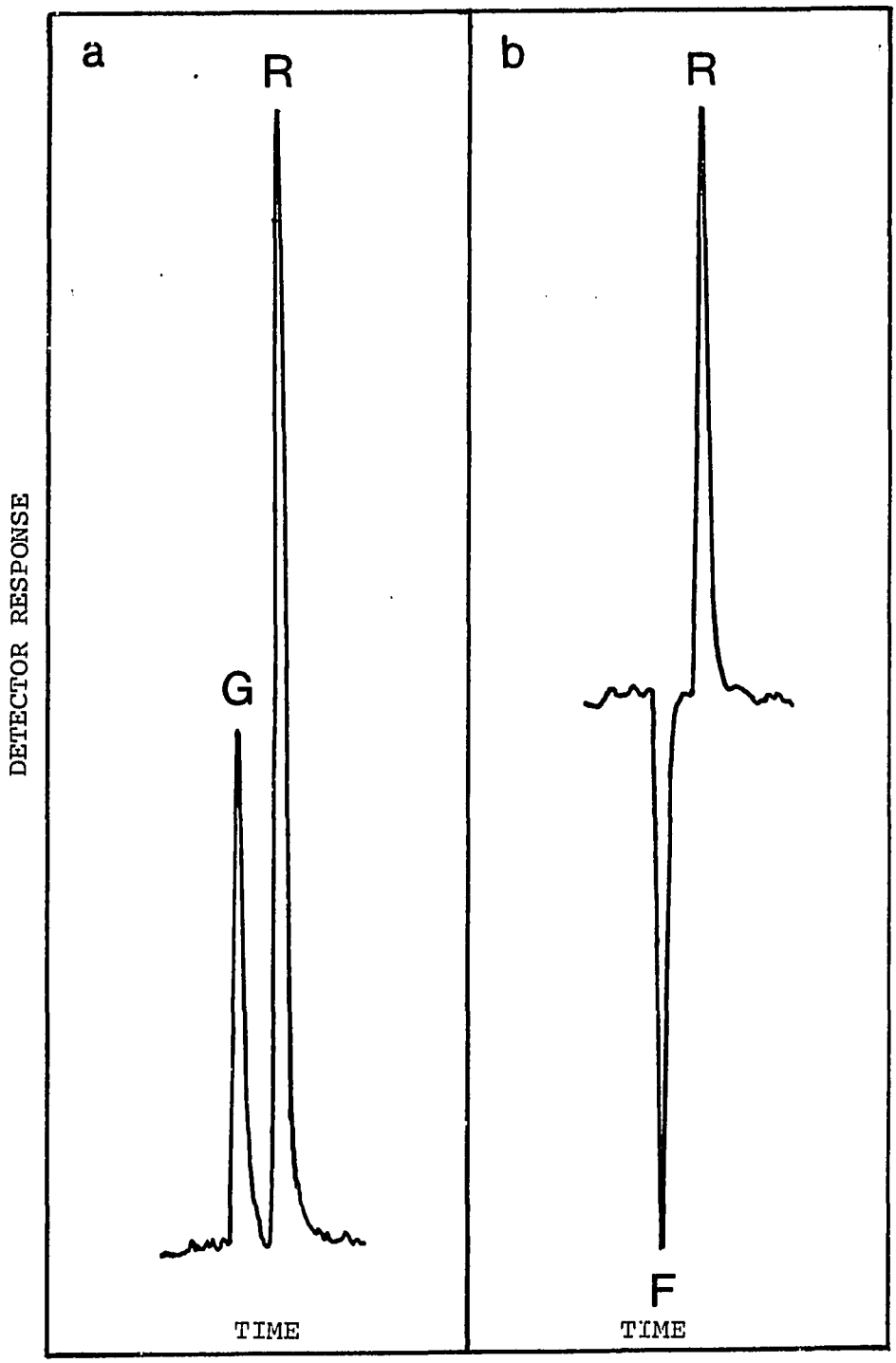
a
R
G
TIME
b
R
F
TIME
DETECTOR RESPONSE

and raffinose. The peaks go up or down depending on whether the species is dextrorotatory or levorotatory, respectively. Also, the peak heights of the sugars are found to be in proportion to their respective specific rotation as would be expected from equal amount injection. It is clear that we are observing the correct effect. The detection limits of these sugars in water, based on a S/N of 3, were estimated to be 0.5 μg. This represents a significant improvement in detectability when compared with the commonly used RI detector. Since the above results were obtained in the early stage of this work, there is still room for improvement. To lower the detection limit, it is imperative to improve the signal-to-noise ratio (S/N) by either noise reduction or signal enhancement, or both simultaneously.

According to Equation 6, it is possible to increase the signal by increasing the modulation angle α through a larger magnetic field (larger coil current) or longer light path in the Faraday rotator without increasing the noise level. To increase the efficiency of the modulation driver, the 10-cm long first generation modulating Faraday rotator (identical to the compensating Faraday rotator) was replaced by two matched 20-cm long modulating Faraday rotators (described in the experimental section) with windings in the opposite directions. Each member of this pair was thus

driven during alternate half-cycles of the square wave. This arrangement also guaranteed that electronic zero was always maintained in the lock-in-amplifier and that the point of maximum extinction with the two modulators off was the best setting for the analyzing polarizer. The modulating angle was effectively four times that used previously when the same magnetic field strength was applied.

The dependence of signal enhancement on the magnitude of modulation angle is shown in Figure 6, where a constant signal corresponding to a 3×10^{-4} degree magnetic rotation is introduced to check the signal to noise ratio performance. For each comparison, three distinctive voltages of 50, 100, and 150 volts were applied to the modulating Faraday rotators against that constant Faraday rotation. It can be easily observed that a linear relationship exists between S/N and modulation angle as would be expected from Equation 6. However, there is a practical limit for air-based Faraday rotators to perform large modulation. Dictated by the low Verdet constant of the air, one needs to invest a higher degree of instrumental sophistication to overcome the problem associated with high current switching; like the dissipation of ohmic heat generated in the solenoid and the availability of a high voltage, high current dc power supply. Another approach might be through the development of a mobile phase-based Faraday rotator to

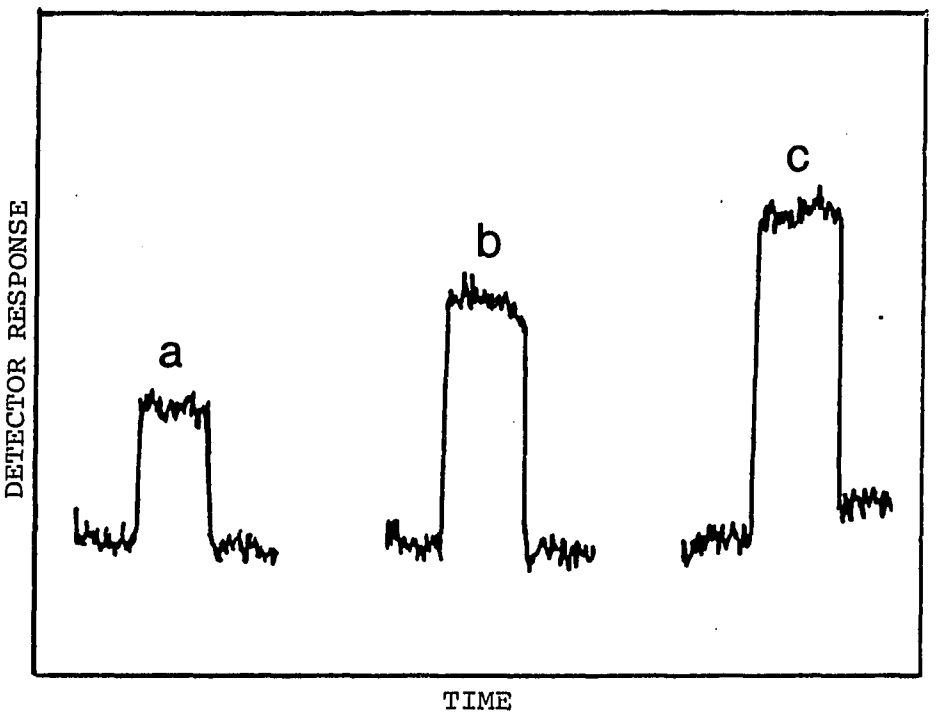

Figure 6. The signal-to-noise ratio of a constant magnetic rotation ($3x10^{-4}$ degrees) as a function of applied voltage (modulation angle) across the 20-cm long air-based Faraday rotators, laser power, 20 mW at 514.5 nm; lock-in amplifier time constant, 1 second ((a) 50V, (b) 100V, (c) 150 V)

take advantage of the high Verdet constants of the liquids.

The noise performance can not be quantitatively characterized, since it is normally a complex composite with contributions from the mechanical, electrical, chemical, and optical sources in this system. For example, it was expected that a factor of N increase in the laser power would translate into a corresponding $\sqrt{N}$ factor improvement in S/N according to the principle of signal averaging (73). However, in practice, the improvement (see Figure 7), is only marginal in our system due to a variety of reasons. First, laser heating causes changes in birefringence in the polarizing crystals as well as the cell windows. Secondly, when the two polarizers were crossed, the light entering the second polarizer (the analyzer) is rejected almost totally to the extent of the extinction ratio. The rejected light heats up the surrounding cement which holds the polarizing crystal in position. The thermal relaxation in the cement causes the crystal to rotate minutely and it randomly deviates from the chosen best extinction. Thirdly, with the flow cell in place, the light beam diverges due to the thermal lens effect (41), caused by the absorption process in the organic mobile phase. The expanded beam size reduces the effectiveness of the extinction. These three effects combine to increase the level of residual depolarized light through

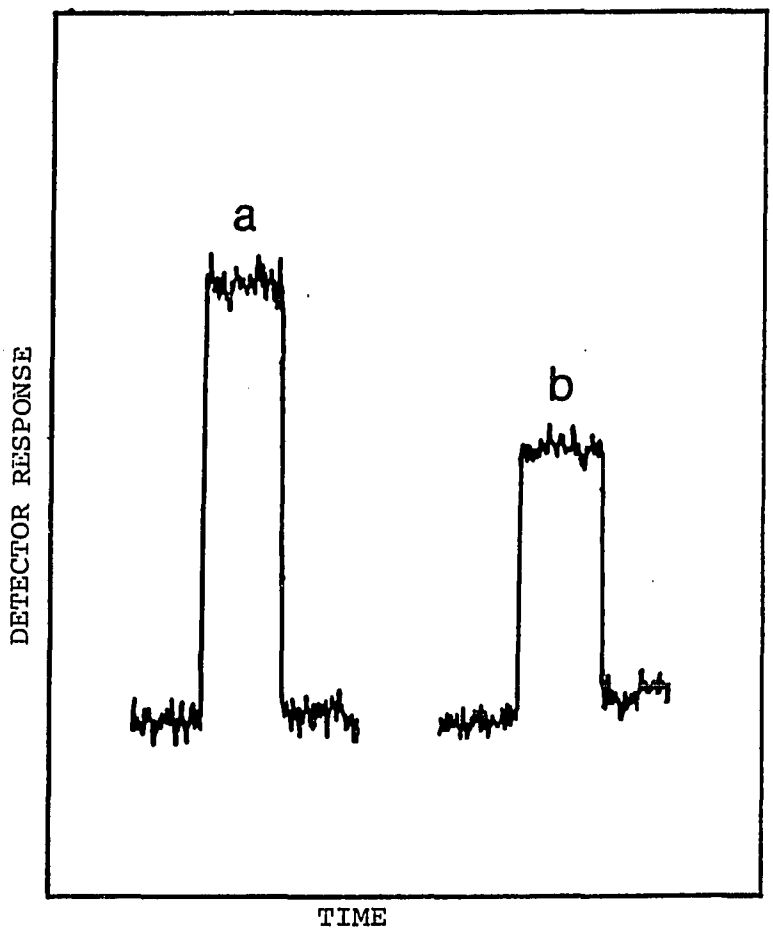

Figure 7. The signal-to-noise ratio of a constant magnetic rotation (3×10^{-4} degrees) as a function of laser power (514.5 nm) lock-in amplifier time constant, 1 second ((a) 40 mW, (b) 20 mW)

the crossed polarizers in addition to the other major sources of residual light coming from the imperfect extinction, light scattering and system birefringence. Even though this kind of radiation is not modulated, it increases the mean level of light intensity, which contributes a proportional increase in shot noise but no signal enhancement in the output of the photomultiplier tube. The performance of the lock-in amplifier was degraded with a poor signal-to-noise ratio as a result. Since both heating and thermal lensing effects are laser-power dependent, lower laser powers on the level of tens of mW are most desirable, up to the limit of photon statistics.

It is also important to isolate the system from vibration which would cause rotational displacement of any of the polarizer, analyzer (both are mounted in rotational stages), and flow cell relative to any of the others on the order of 10^{-3} degrees. Misalignment of the beam steering optics (i.e., the laser, mirrors and lens) could also adversely add significant noise to the output, thereby, substantially affecting the operation of this system. Isolation from such vibration is generally possible by simply using a very rigid table like a breadboard. However, if needed, a vibration-isolated optical table equipped with three free standing pneumatic isolation mounts for vibration

isolation and self-leveling can be used.

The flow cell is the most critical component for the optimization of the S/N. Bubbles trapped inside the cell, particularly when the new windows are installed, will cause light scattering problems. We find that as long as cell walls and windows remain "wetted", bubbles do not seem to accumulate. Also, misalignment of the cell increases the noise level substantially. This is due to scattering and reflections off the cell walls and the off-normal incidence angle at the cell windows, so that depolarization occurs. To a lesser extent, the residual eluent pulsation caused by the action of the reciprocating piston pump equipped with a pulse dampener will distort the cell windows minutely and thus, introduce pumping noise. A more sophisticated solvent delivery system capable of pulseless operation would alleviate this problem significantly.

In assessing the viability of an optical activity detector for HPLC, one of the most important factors to be considered is the detection limit. Single component injections of sucrose in water were performed to evaluate the detection limit and linearity response. A combined chromatogram showing the detector responses of 5.0, 1.0, and 0.1 μg sucrose injected into a standard 10-μm C_{18} column using water as eluent is shown in Figure 8. A

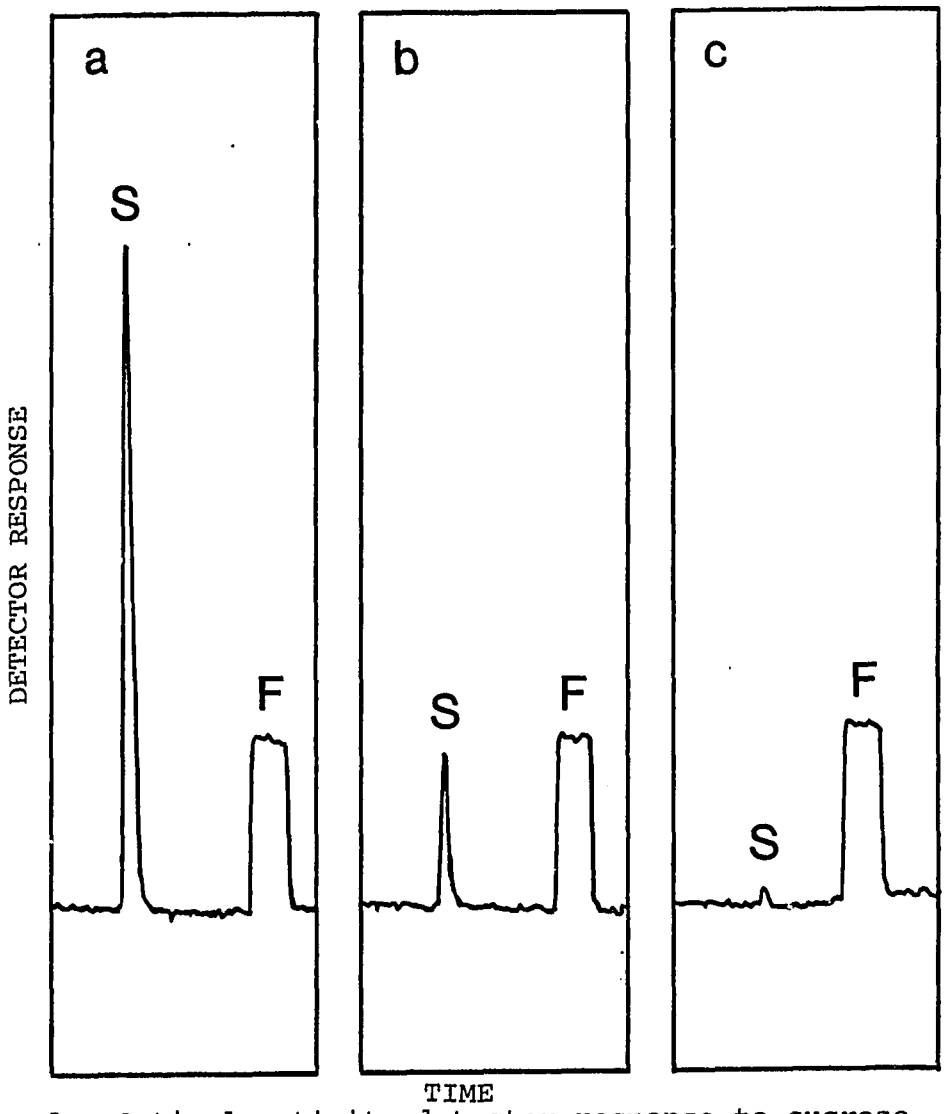

Figure 8. Optical activity detector response to sucrose injection ((a) 5.0 µg, (b) 1.0 µg, (c) 0.1 µg - mobile phase, water; flow rate, 1 mL/min; LC column, 10-µm C_{18}; lock-in amplifier time constant, 3 second; S, sucrose; F, Faraday rotation, 3×10^{-4} degrees)

A detectability of 100 ng sucrose which has an optical rotation of $2x10^{-5}$ degrees, is obtained based on the signal-to-noise ratio of 3. For compounds with large specific rotations and/or detected at shorter wavelengths, the detection limit can be significantly lower.

The peaks in the square-wave form as shown in the same chromatogram were generated by applying 0.25 amperes of constant current over some period of time across the compensating Faraday rotator. The magnitude of the Faraday rotation, using air as the medium, was calculated to be about $3x10^{-4}$ degrees. This method not only removes the need and inconvenience of injecting internal standards into the chromatographic system for calibration purposes but also provides a quick, reliable, and efficient means of checking system performance. It was found that linear response to concentration is achieved over the 2 orders of magnitude of the concentration tested with absolute amounts of sugar injected ranging from 0.1 μg to 20 μg.

In view of the much improved sensitivity in our optical rotation measurement HPLC system, as demonstrated in this chapter, we can envision the potential of its application to a wide variety of research areas. The low detection limit coupled with the high degree of selectivity will enable the optically active compounds to be separated and detected in a

complex matrix of other compounds such as is frequently encountered in natural product extracts, or in biological fluids.

CHAPTER IV. DETERMINATION OF CARBOHYDRATES IN URINE BY HPLC AND OPTICAL ACTIVITY DETECTION

Introduction

The concept that every individual has its own metabolic profile, reflected in the composition of his body fluids, has been well recognized in biomedical sciences (81). The identification and the determination of the hundreds of compounds that are present in body fluids have been beneficial to establishing pathological conditions (82), understanding the molecular basis of diseases, monitoring the therapeutic effects of drugs (83), and maintaining proper mental health (84). Except for the class of highly specific systems, such as enzyme-substrate or antigen-antibody reactions, the body fluids are in general too complex to be analyzed without some sort of separation scheme. Very high resolution has been achieved in liquid chromatography for such samples (85,86), but a combination of slow eluent gradient and small particle sizes for the packing material requires an analysis time of the order of many hours. For physiological profiling and for routine clinical usage, these analysis times are prohibitive. It is much more desirable to restrict the studies to individual classes of compounds, so that a simpler, more specific separation procedure can be performed. Or, in cases where sample manipulation needs to

be reduced to a minimum, selective detection schemes for liquid chromatography can be employed to minimize interferences.

Carbohydrates, along with nucleic acids, proteins, and lipids, constitute the four major classes of organic compounds essential to life. The formation of coal, peat, and petroleum can be traced back to the microbiological and chemical conversion of carbohydrates (87). Carbohydrates are also the fuel of life, accounting for some 40 percent of the calorie intake of the human body. These major constituents of the human diet include glucose, fructose, lactose (milk sugar, a disaccharide of glucose and galactose), sucrose and starch (87). Many of the hereditary or genetic diseases of human beings for which the molecular basis has been established stem from defects of carbohydrate metabolism, mostly of the complex saccharides (88).

The carbohydrates that are present in body fluids are clearly related to metabolic processes in general and their profiling should offer a wide variety of possible uses in diagnostic studies. Much attention has been given to the routine clinical screening for glucose (89) because of the disease of diabetes mellitus.

Several uses of carbohydrates other than glucose for physiological profiling are known. Excess fructose in urine

can be a sign of an inherited metabolic defect (90). Lactose is present in urine in late pregnancy and during lactation, but excess can indicate a rare metabolic disease (91). The inherited disease galactosemia causes the presence of galactose in urine, but galactose can also be an indication of severe hepatitis or biliary atresia in neonatal infants (91). The last condition can lead to liver damage, mental retardation, and cataracts. The presence of xylose is related to yet other familial disorders (92). The xylose absorption test can be used to diagnose either enterogenous steatorrhea (93) or kidney malfunction. Since the carbohydrates are directly involved in the metabolic cycles of the body, one would expect dietary and metabolic deficiencies to affect carbohydrate profiles in serum and in urine. It is therefore important to have reliable methods for analysis, so that correlations can be studied.

For glucose determination the accepted method using hexokinase (94) in relatively free from interferences, but requires 500 µL of protein-free filtrate. This can become impractical for fetal or pediatric applications. The other simple sugars are often neglected, primarily because of the lack of reliable quantitative methods at the low concentration levels typical of body fluids. Paper chromatography provides qualitative information in a reasonable time (95, 96), but even semi-quantitative results are difficult to

obtain at these concentrations. Automated high-resolution analyzers with sensitivities in the μg range have been used to study carbohydrates in body fluids (97, 98), but again hours are required per analysis. More recently, cation exchange resins have been successfully used for separating dextrose and fructose from the higher saccharides in food products (99), but the limitation on sensitivity make the scheme unsuitable for studying body fluids. The use of a refractive index detector in these cases is dictated by the lack of convenient UV absorption bands for the carbohydrates, and is a particularly weak link since the columns must be operated at above-ambient temperatures. Post-column colorimetric methods have been used (100), but should be avoided if more reliable and faster methods can be found. Flame ionization detectors have been used (101), but again are not sensitive enough.

Electrochemical detection of carbohydrates separated by HPLC has been successfully demonstrated in real samples (102). Application of triple pulse amperometry at a platinum wire-tip electrode resulted in the 0.5 μg detectability for glucose and similar sugars. However, the compatibility among eluent composition, pH, electrode material, temperature, and column packing must be closely matched.

A detector for HPLC that is particularly suitable for

carbohydrate analysis is one based on the optical activity of these compounds. This detector eliminates most of the restrictions on the choice of eluents and gradients as well as change in temperature so that the chromatography can be optimized independently. A procedure for the HPLC separation and optical detection of urinary sugars will be described in this chapter.

Experimental

Chromatography

Separations were performed on a heavy metal cation exchange column that is commercially available (Bio-Rad Laboratories, Richmond, Ca., HPX-85 Heavy Metal). This column has been optimized for the monosaccharides. The operating conditions were as recommended by the manufacturer, i.e., water at a flow rate of 0.64 mL/min was used as the eluent and the column was maintained at 85°C with a home-built water jacket. All injections were through a 100 μL loop at a conventional injection valve (Rheodyne, Berkeley, Ca., Model 7010). To reduce any pressure fluctuations caused by the pump (Milton Roy, Riviera Beach, Fla., Model 196-0066-001) at the detector, we used a commercial pulse-dampener (Alltech, Deerfield, Ill., Model 9404) in conjunction with a pressure gauge (Alltech, Arlington Heights, Ill., Model 9228). Pressure fluctuations were further re-

duced as a result of having a UV absorbance detector (Spectra Physics Chromatronix, Santa Clara, Ca., Model 210) in series and before the optical activity detector. Since the flow-cell was essentially at room temperature, the eluant must be cooled to some extent from 85°C so that turbulence would not exist in the cell. It was found that having the UV detector in series was sufficient for cooling. Alternately, a 50 cm length of standard chromatographic stainless steel tubing was also satisfactory. Cooling or temperature control, however, was not as critical as in a refractive index detector. Test solutions were all reagent grade material (Fisher Scientific, Fair Lawn, N.J.) dissolved in deionized water. To protect the chromatographic column, urine samples were passed through a mixed-bed (Mallinckrodt Inc., Paris, Ky., Amberlite MB-3) ion exchange column, but otherwise untreated. Identical protection can be achieved using a commercial guard column, so that pretreatment is eliminated from the procedure.

Optical activity detector

The basic arrangement for an optical activity detector for HPLC has been reported earlier in Chapter III. In this work, the laser was operated at 488 nm to better match the spectral response of the photomultiplier tube and to take advantage of the slightly larger specific rotations of these

compounds, although these differences are minimal. Since it was found previously (78) that a major source of noise is shot noise from the incompletely extinguished laser beam in the absence of a sample, we introduced intensity stabilization in the laser. This was accomplished by passing the laser light through a Pockels cell (Lasermetrics, Teaneck, N.J., Model 3030) and then a Glan prism (Karl Lambrecht, Chicago, Ill., Model MGLS-DW-8) aligned slightly off-axis from the polarization direction of the laser. A photodiode was used to monitor the intensity after this arrangement. After proper amplification, the signal was compared with an adjustable reference level, so that an error signal could be generated. A high voltage operation amplifier (Burleigh Instruments, E. Rochester, N.Y., Model PZ-70) then provided feedback to the Pockels cell to control the intensity. The intensity stabilization improved the signal-to-noise ratio and avoided drifting in the baseline in the chromatograms.

The internal volume of the flow cell has been reduced to 80 μL by using a smaller drill-bit without any adverse effects, as predicted in the earlier work (78). It was found that the cell windows were useful for months unless they were contaminated by the chromatographic effluent, as evidenced by visible deposits. The position of the cell in

the optical path was such that the laser beam cleared the cell walls, since scattering caused depolarization. The cell windows were installed for a given position of the cell, but only occasional, minor adjustments by the cell positioner was needed over the period of a week. The entire assembly was mounted on a 2-inch thick optical breadboard (Newport, Fountain Valley, Ca., Model LS-48) on a conventional laboratory bench, since we found that sophisticated vibration isolation was not needed.

For the feasibility studies using the He-Ne laser (Spectra Physics, Mountain View, Ca., Model 134), a 2X beam expander based on a Galilian telescope was used before the focusing lens so that the proper beam-waist can be achieved at the cell. In that case, an Amperex 56TVP photo-tube (North American Philips, Hicksville, N.Y.) was used to provide a better spectral response.

Results and Discussion

A chromatogram showing the separation of optically-active components in untreated human urine using a 10-μm C_{18} reversed-phase column (78) is shown in Figure 9. The first components show up at the 2-min point and include all of the unretained species. Due to the lack of retention, a high concentration of material passes through over a short

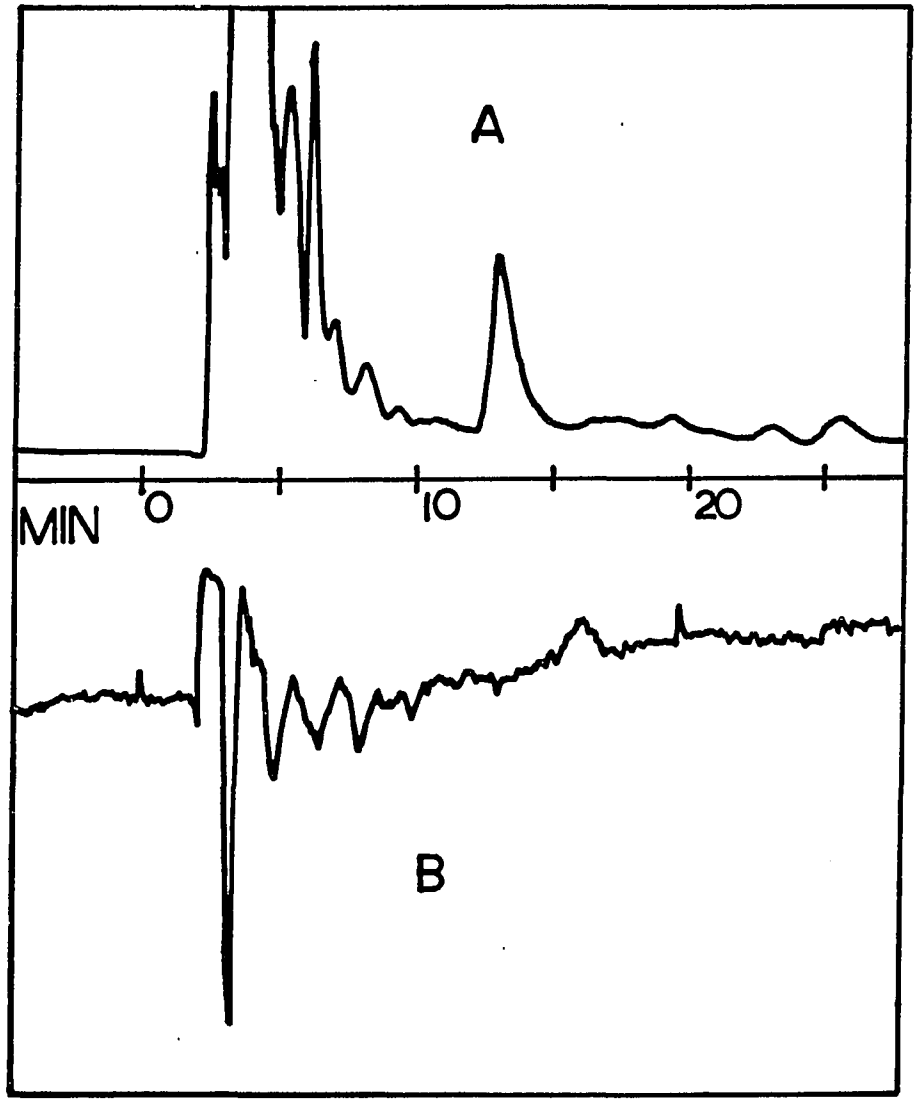

Figure 9. Separation of components in untreated human urine by a 10- μm C_{18} reversed-phase column (A, absorption detector at 254 nm; B, optical activity detector. Water is the eluent with flow rate at 1.0 mL/min)

period of time that refractive index and thermal lensing effects dominate the matter-radiation interaction. The laser beam is both deflected and distorted and will not pass through the analyzer and the apertures properly. It was observed that the same urine sample with 100-fold dilution did not create any disturbance, but a lot of features disappeared except the glucose peak.

To increase the retention and improve chromatographic efficiency, two 10-μm C_{18} reversed-phase columns were connected in series for the same urine study. The chromatogram shown in Figure 10 is a substantial improvement over the earlier work. Again, the second major positive feature, which was off-scale, was accompanied by turbulence in the flow cell caused by the large refractive index change. Even though the sugars and cysteine are the only components positively identified, one can see that potentially useful information is present, particularly since very few of these features also show up in the UV detector. These preliminary findings point to the need for different chromatographic conditions if meaningful quantitative results are to evolve from this study.

The Aminex HPX-85 heavy metal form column is chosen because it is specifically dedicated to carbohydrate analysis. This newly developed column, packed with heavy

Figure 10. Separation of components in human urine using two 10-μm C_{18} reversed-phase columns in series and optical activity detector (Peaks: C, cysteine; M, monosaccharides; D, disaccharides; T, trisaccharides. Water is the eluent with flow rate at 1.0 ml/min)

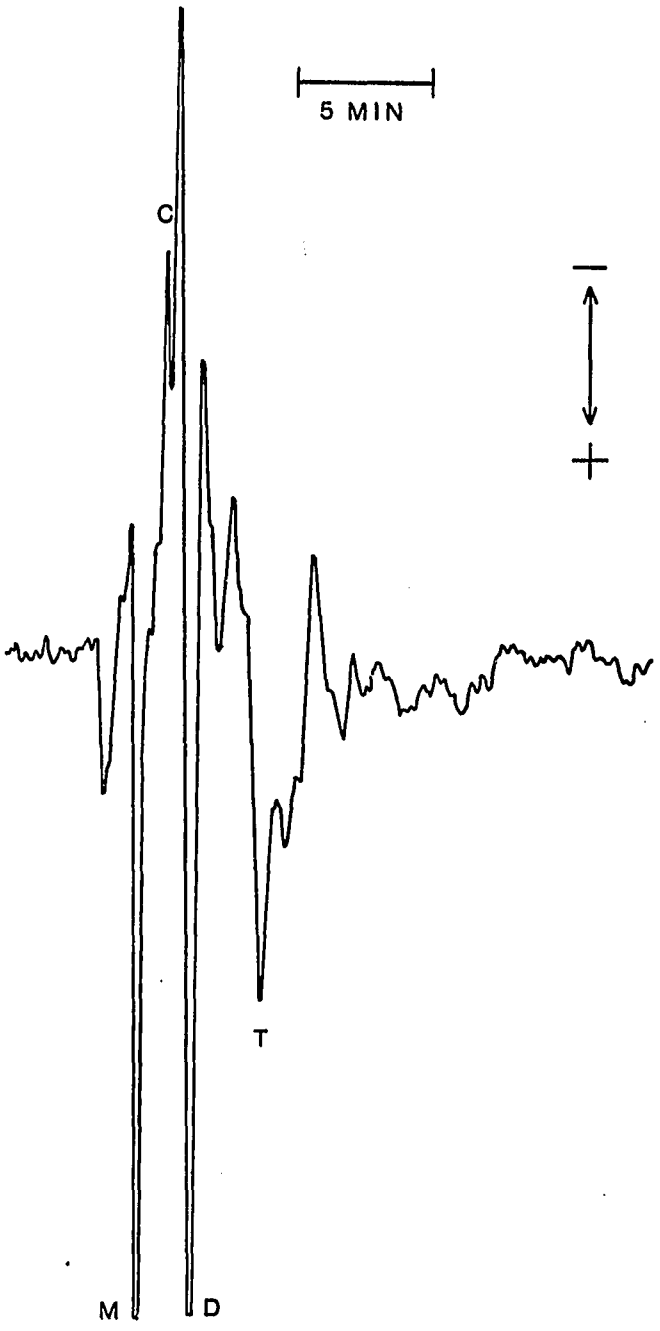
5 MIN
C
T
M
D

metal form 8% crosslinked polystyrene cation exchange resin, is highly selective and also optimized for separation of monosaccharides as typically found in human urine. The ionic nature and high cost of this column (about $500 per column) demand prior sample preparation before direct urine sample injection to safeguard the column and guarantee optimum performance. Substances with a high positive charge, such as sodium, potassium, or amino acids, will bind tightly to a cation exchange resin and are therefore trapped by the column. Substances with a high negative charge, such as chloride ions, are excluded from the packing material and elute at void volume and contribute to the creation of a disturbance in the flow cell. Since the above-mentioned ionic species are abundant in human urine (103), it is necessary to employ a mixed-bed ion exchange column for their removal but without a corresponding effect on carbohydrates.

All the separations on the Aminex HPX-85 Carbohydrate Analysis Column were performed under the same, straightforward conditions: at 85°C temperature, with water as eluent, and at flow rate of 0.64 mL/min as recommended by the manufacturer. The urinary sugars are mostly monosaccharides which are quite similar in molecular structure and properties. For this group of compounds to be satisfactorily resolved, significant gain in separating power

would offer markedly improved performance. A low-viscosity solvent tends to give a higher column efficiency as the kinetic processes within the column are improved. For many liquids the viscosity decreases with temperature in a near linear fashion. Graphs which are constructed by plotting viscosity against temperature for water, our chosen mobile phase and a comparatively viscous solvent, show a factor of approximately three reduction in viscosity (from about 1 down to about 0.33 centiposes) over the temperature range from ambient to 85°C (7). It is expected that the column efficiency will improve in a similar manner. Working at high temperature can also improve the solubility of the sample components, and lead to reduction in the inlet pressure. In this work, circulating water jackets made of copper were used to control column temperature. The temperature monitor was an Omega type K Chromel-Alumel thermocouple (Omega Engineering Inc., Stamford, Conn.). One end of the thermocouple was pressed on the copper surface with soft indium metal which was then clamped on the water jacket to maintain good thermal contant. The whole set-up was wrapped with asbestos tape for insulation. The reference junction was kept at a temperature of 0°C (ice water) and the voltage at the other end was monitored through a digital voltmeter. A 3.5 volt reading signals

a temperature of 85° at the water jacket as boiling water was circulating through it. The flow rate controlled by a peristaltic pump dictates the equilibrium temperature. The temperature control was within ± 2°C. The chosen mobile phase flow rate represents a compromise between long retention time and increased efficiency in a resin packed column. This also prevents excessive backpressure and breakdown in peak symmetry.

Test solutions of individual sugars were run to determine the retention times under our experimental conditions. In general, the order of elution and chromatographic efficiency was as specified by the manufacturer. No effort to further optimize was made. The results of the analysis of human urine are shown in Figure 11. We have identified six urinary carbohydrates, based on the specificity of this column, retention times as correlated to injection of test solutions of sugars, the lack of UV absorption at the corresponding locations, the sign and magnitude of the individual specific rotation, and the estimated concentration levels in normal human urine (97). The last comparison is shown in Table 1, with the method for calculation given below. It is clear that determination of these carbohydrates as outlined here, presents no problem. The peaks that appear prior to sucrose represent the unretained

Figure 11. Separation of components in human urine by HPX-87 hevay metal column ((A) UV detector, (B) optical activity detector), (S, sucrose; L, lactose; G, glucose; X, xylose; A, arabinose; F, fructose. Water is the eluent with flow rate at 0.64 ml/min and operating temperature at 85°C)

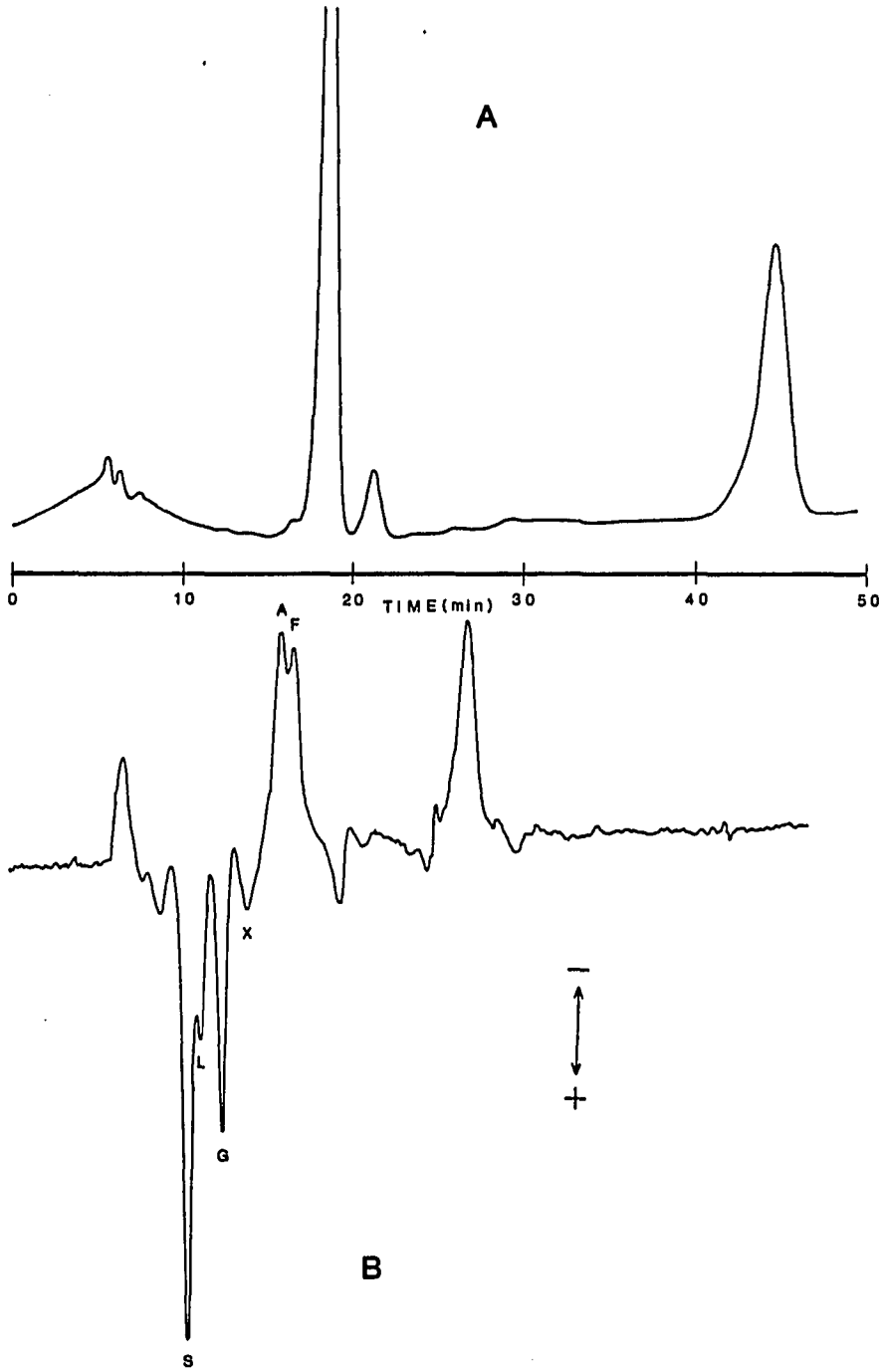
A
0
10
20
TIME(min)
30
40
50
A
F
X
L
G
S
B

Table 1. Concentrations of sugars in urine

	Concentration (μg/mL)[a]		
	This work	Reference (97)	Normal range
Sucrose	22	12	0-50
Lactose	10	49	0-100
Glucose	16	24	10-120
Xylose	10	10	0-30
Arabinose	7	26	0-30
Fructose	7	2.7	0-50

[a]All concentrations are ± 10%.

components and the higher saccharides, in that order. The major feature at 27 minutes does not seem to correlate with any of the carbohydrates tested, although one would expect species similar to mannitol and sorbitol to elute about then. It is interesting to note that the three major features in the UV detector correspond to a shoulder, a minor feature, and nothing at all in the optical activity detector. This emphasizes the substantial differences in the two detectors for studies in biological fluids. The UV peaks also indicate that even if a refractive index detector

can approach this level of sensitivity, additional interferences will be present and limit its usefulness. The chromatographic efficiency can probably be further increased by lowering the flow rate, or by connecting a second column in series, but the simplicity of the chromatogram makes such a compromise with the analysis time not necessary.

Calculations of the concentrations are straightforward. Although, naturally, standards must be used for checking, one can use the absolute standard given by a d.c. Faraday cell of known properties at a known current. In this work we used a current of 0.25 A to produce a field of 250 G. With air, this corresponds to a net rotation of 0.28 millidegrees. Using the specific rotations [α] for the Na D line, which is not too different for this wavelength, one has:

$$c = \frac{\alpha}{[\alpha]} \qquad (7)$$

where c is the concentration in grams per mL, and α is determined by the ratio of the peak height and the effective height of the d.c. Faraday rotation, multiplied by 0.28 millidegrees, since our cell is 1 dm in length. The $[\alpha]_D$ values were used taking into account mutarotation. The peaks in Figure 11 are typically in an eluant volume much

larger than that of the flow-cell, so that a triangular approximation can be used for the area. Conversion to total quantity injected is then simple, knowing that the flow rate is 0.64 mL/min. Since the chromatography was highly reproducible, one could deconvolute the overlapping features if desired. However, the fluctuations in human urine did not warrant such an attempt at high accuracy in this work, and the simple triangular approximation was used. The results of this particular urine sample are presented in Table 1, together with some other reference values (10). We find that the determined values are reasonable. For routine applications, one would probably rely on peak height measurements established by standard solutions, rather than use the absolute standard method described here.

In the course of identifying sources of noise, we used a 2 mW He-Ne laser as the light source in place of the argon ion laser. There is much more short term fluctuation in the He-Ne laser, so that the intensity cannot be stabilized as well. The lower light level also makes it more difficult to identify sources of stray light and to eliminate them. Even with these problems, we were able to obtain a detectability of 1 μg (S/N = 3) for fructose under the same conditions. This demonstrates that photon statistics was not the limiting factor in detectability in the

case of the argon ion laser. For the He-Ne laser, however, photon statistics was a major contribution. We estimate that a laser with a power of 10-50 mW can be used instead of the expensive argon ion laser without sacrificing performance. We also found that when the lower power laser was used, the system took less time to warm up. This is because heating causes changes in birefringence in the polarizing crystals as well as the cell windows, and lower laser powers are desirable, up to the photon statistics limit.

In summary, it is clear that in the detection of optically active components separated by HPLC, the detectability of 100 ng is sufficiently sensitive for the study of urinary carbohydrates, particularly the monosaccharides. This allows the simultaneous determination of six naturally occurring carbohydrates in a 100-μL sample of human urine, which is injected directly except for a simple deionization step. The reproducibility and reliability of this method should allow better insight into the relation between urinary sugars and various physiological conditions.

CHAPTER V. DETERMINATION OF FREE AND ESTERIFIED CHOLESTEROL IN HUMAN SERUM BY HPLC AND OPTICAL ACTIVITY DETECTION

Introduction

Cholesterol, a major component of all mammalian plasma membranes, is vital to cell growth and survival (104, 105). It belongs to a subgroup of steroids called sterols and is the biological precursor of some of the steroids. One of its physiological functions is to provide a storehouse of perhydrocyclopentenophenanthrene rings to which other groups can be introduced via biosynthesis to become usable steroids (106). The ring skeleton of cholesterol contains 27 carbon atoms and eight of them are chiral centers. Although the molecular structure is complex, the biosynthesis of the total molecule is accomplished from relatively simple acetate units. Consequently, many amino acids, carbohydrates, and fatty acids, when supplied in excess of other metabolic needs, can contribute to the cholesterol pool (107). Excessive amounts of cholesterol can deposit in the inner layers of large arteries and contribute to the development of atherosclerosis (108). The accumulation of these liquids in major arteries can restrict the flow of blood to vital organs and eventually lead to heart attack or stroke.

Cholesterol is found in two forms in the serum: either

as free cholesterol, or esterified with a long chain fatty acid such as palmitic acid. Typically, about 75% of the serum cholesterol is esterified (109). This ratio has been shown to be related to hormones (110), diet (111), toxic conditions such as ethanol poisoning (112), and disorders like familial lecithin:cholesterol acyltransferase deficiency (113).

Numerous analytical procedures are available and are being used for the measurement of serum cholesterol because of its clinical significance. The most commonly used methods are photometrical and based on the color reaction of cholesterol with acid reagent (107). The Liebermann-Burchard method, or a modification of it, has been the most popular procedure, which consists of mixing a chloroform or acetic acid solution of cholesterol with concentrated sulfuric acid in acetic anhydride. Depending on the relative concentration of sulfuric acid, and the presence or absence of ferric ion, one can obtain either a green color (λ_{max} = 410 nm) or a red (λ_{max} = 563 nm) (107). Disadvantages of the colorimetric methods include temperature dependence, light sensitivity, color instability, nonspecificity as well as the manipulation of corrosive reagents (109). Various different colorimetric methods for the analysis of serum cholesterol has been reviewed and critically evaluated (112).

The first step in the newer enzymatic method involves

the catalyzed hydrolysis of the cholesterol esters by cholesterol ester hydrolase to generate free cholesterol, which is oxidized to 4-cholesten-4-one and hydrogen peroxide. The hydrogen peroxide thus can be related to the total cholesterol (113). This method is highly accurate and inherently specific but is mainly for total serum cholesterol determinations.

Among other methods, various chromatographic techniques have also been applied for serum cholesterol analysis. In thin-layer chromatography (TLC), cholesterol and its esters are separated from other serum lipids on a silica gel coated thin-layer plate, the chromatogram is stained for color development and the bands are scanned using a densitometer (114, 115). This direct method lacks the necessary precision. In the indirect but very tedious approach (116), the separated cholesterol fractions are eluted from the silica gel and are quantitated by some conventional method. For the quantitative determination of the total cholesterol by TLC direct method, the cholesterol and its esters can be separated from other lipids by double extraction, using a combination of alkaline, alkaline isopropanol and n-octane (117). This is needed since the color-producing reaction is not specific for cholesterol. Triglycerides, free fatty acids and

phospholipids are the major interferences.

Gas-liquid chromatography (GLC) has been gaining wider acceptance for serum cholesterol analysis and has given accurate and reproducible analysis for both free and total cholesterol determination. Free cholesterol can be quantified directly from a serum extract prepared according to the procedure of Folch et al. (118) and by using butanol-diisopropyl ether (119). For analyzing total cholesterol the serum samples were saponified and extracted following the Abell-Kendall method (120). The ethanolic KOH is used for releasing cholesterol from the lipoprotein complexes and for hydrolyzing cholesterol from its esters in the saponification step. The free cholesterol is then extracted into petroleum ether or hexane. The amount of original esterified cholesterol is then determined by the difference of the two measurements. An isotope dilution-mass fragmentography technique has been applied for the GLC analysis of total serum cholesterol (121). Both liquid phase packed columns and capillary columns have been used. The mode of mass spectrometry detection can be electron impact or chemical ionization depending on the types of labelled isotopic internal standard.

Cholesterol has no conjugated system but a single double bond within the ring structure (see Figure 12). The fact that cholesterol is presented in serum without

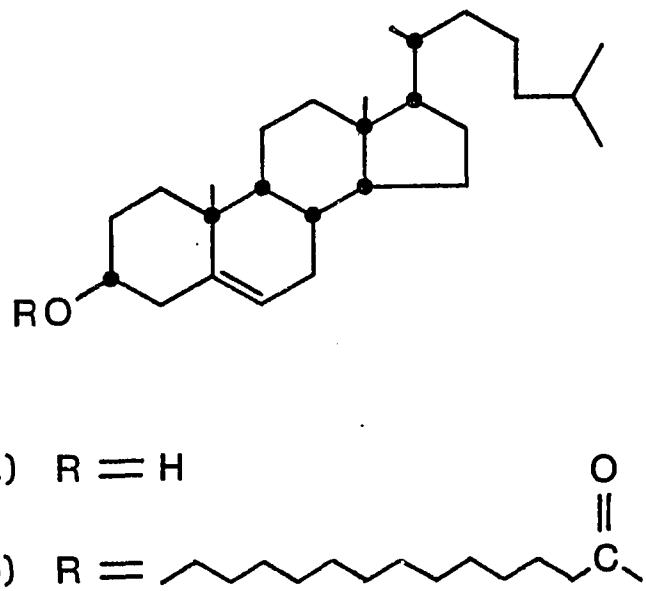

Figure 12. The structural formulas of free (a) and esterified (b) cholesterol showing the eight separate chiral centers

appreciable extinction at 254 nm, the operating wavelength of commercially available UV detectors, creates difficulties in performing liquid chromatographic analysis due to the lack of sensitivity. Recently, the availability of variable wavelength UV detectors in HPLC allowed the determination of both free and esterified forms of cholesterol in a single run (122). Although cholesterol can be detected at 200 nm where double bonds and other functional groups absorb energy, the choice of solvents becomes severely limited due to the transparency requirement in this region. Also, more interferring compounds would absorb and be detected at this short wavelength. A particularly serious problem is the interference from triglycerides (122). This makes good separation and accurate quantitation difficult.

We describe here an alternative procedure for the reversed-phase HPLC separation and determination of free and esterified cholesterol as it is found in human serum by on-line monitoring of the optical rotation of the eluate. The combined use of simple extraction, direct sample injection, HPLC and optical activity detection offers a sensitive and specific method for the profiling and quantitative analysis of serum cholesterol and its esters.

Experimental

Chromatography

Separation was performed on a 25 cm x 4.6 mm, 10-µm C_{18} column (Alltech, Deerfield, Ill., U.S.A.). Samples were eluted with a tetrahydrofuran-water (76:24, v/v) mobile phase at a flow rate of 0.5 ml/min and a pressure of about 650 psi. All injections were made through a 200-µl sample loop at a conventional injection valve (Rheodyne, Berkeley, Ca., U.S.A., Model 7010). To reduce any pressure fluctuations caused by the pump (Milton Roy, Riviera Beach, Fla., USA, Model 196-0066-001) at the detector, we used a commercial pulse-dampener (Handy & Harman, Norristown, Pa., U.S.A., Model Li-Chroma-Damp II) in conjunction with a pressure gauge (Alltech, Deerfield, Ill., U.S.A., Model 9228).

Materials

Cholesterol and cholesteryl esters were purchased from Sigma (St. Louis, Mo., U.S.A.). Reagent grade tetrahydrofuran was obtained from Fisher Scientific (Fair Lawn, N.J., U.S.A.). Water was deionized locally. Leder Norm normal clinical chemistry control serum was obtained from Lederle Diagnostics (American Cyanamid, Pearl River, N.Y., U.S.A). Reference serum for automated procedures was purchased from

Sigma (St. Louis, Mo., U.S.A., Cat. No. R3626). The serums from the two commercial sources were reconstituted with diluents as instructed by the manufacturers. Fresh serum from a healthy individual was obtained locally. For each 2.4 ml of serum sample, 7.6 ml of tetrahydrofuran was added drop by drop along with vigorous stirring. The mixture was then centrifuged for 20 minutes at 11,000 G (10,000 rpm) in a clinical centrifuge. The clear and yellowish liquid phase was thus separated from the residue and was used as the sample without further treatment. The prepared samples were then injected directly using the chromatographic and detection conditions described in this section.

Optical activity detection

The basic arrangement for an optical activity detector for HPLC has been reported earlier in Chapter III. In this work the laser was operated at 514.5 nm. The laser power was maintained at about 20 mW at the flow cell by replacing one of the mirrors with a partially reflective optical flat. The system was operated without laser intensity stabilization. Instead, a longer time constant of 10 seconds was used at the lock-in amplifier without sacrificing performance. A flow cell with an internal volume of 200 µl was used. Optical alignment was made easier by the 0.0625 inch

diameter cell, which is about one and a half times the size of the laser beam.

Calibration

Calculation of the concentrations of free and esterified cholesterol was straightforward using the procedures described in Chapter IV (123). In using the simple triangular approximation, the accuracy was limited by the measurement of peak base which was defined through extrapolation. Coupled with uncertainties in the specific rotations [α] at this laser wavelength and this solvent, a maximum error of ±10% was assessed on our calculated results. This is confirmed by injecting single-component solutions of known concentrations for each compound studied.

Results and Discussion

Figures 13 and 14 show chromatograms from the reconstituted serum and the freshly extracted natural serum, respectively, analyzed by the above procedure. Test solutions of individual cholesterols in tetrahydrofuran were used to determine the retention times under the same experimental conditions. LC retention times, the sign as well as the magnitude of the individual specific rotation, the possible distribution and structural considerations were the criteria for peak identification. Five major cholesterol

Figure 13. Separation of cholesterol and cholesterol esters in reconstituted serum (Leder Norm) (Peaks: A, cholesterol and cholestanol; B, cholesteryl linolenate and arachidonate; C, cholesteryl palmitoleate and linolate; D, cholesteryl palmitate and oleate; E, cholesteryl stearate; mobile phase, tetrahydrofuran-water (76:24, v/v); flow rate, 0.5 ml/min)

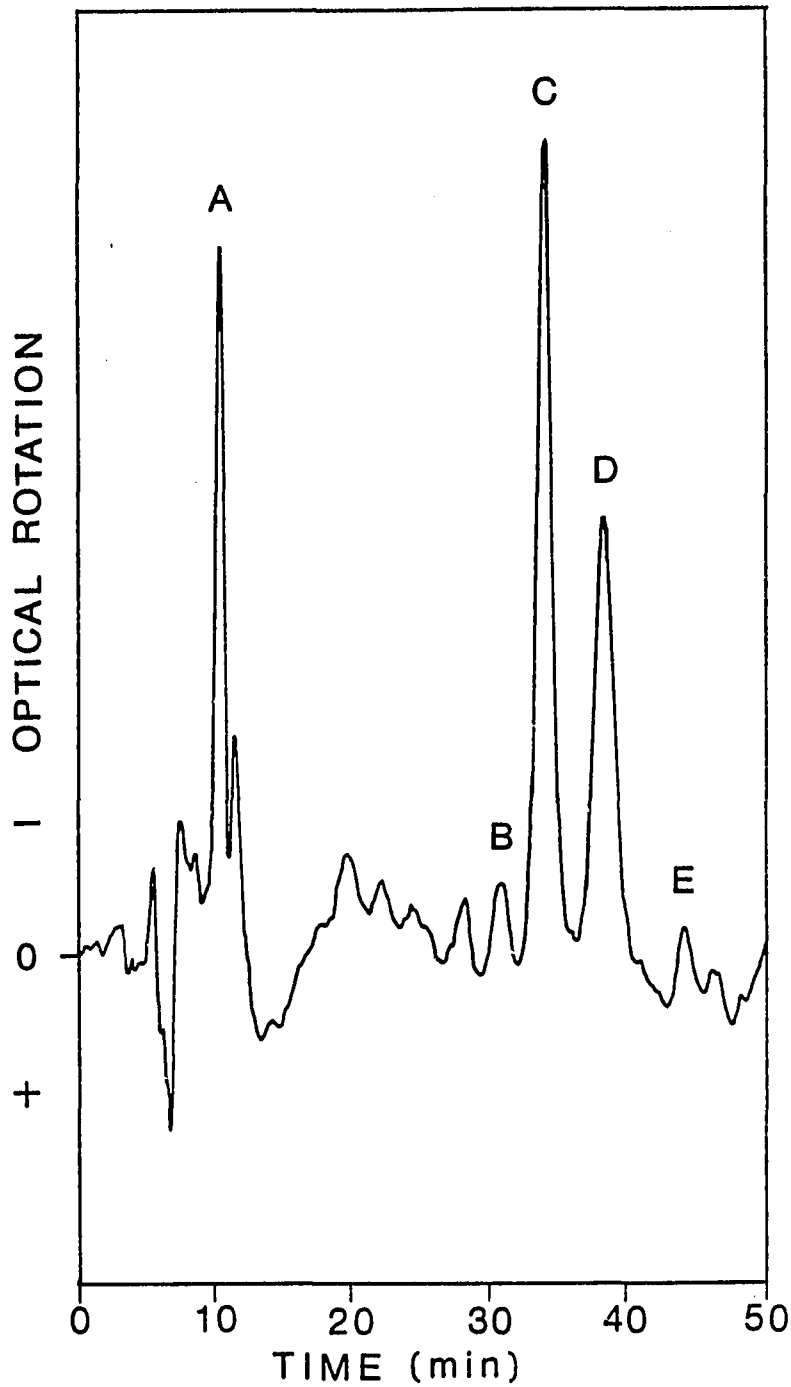
A
B
C
D
E
OPTICAL ROTATION
+
0
−
0
10
20
30
40
50
TIME (min)

Figure 14. Separation of cholesterol and cholesterol esters in natural human serum (local) (Peaks: A, cholesterol and cholestanol; B, cholesteryl linolenate and arachidonate; C, cholesteryl palmitoleate and linoleate; D, cholesteryl palmitate and oleate; E, cholesteryl stearate; mobile phase tetrahydrofuran-water (76:24, v/v); flow rate, 0.5 ml/min)

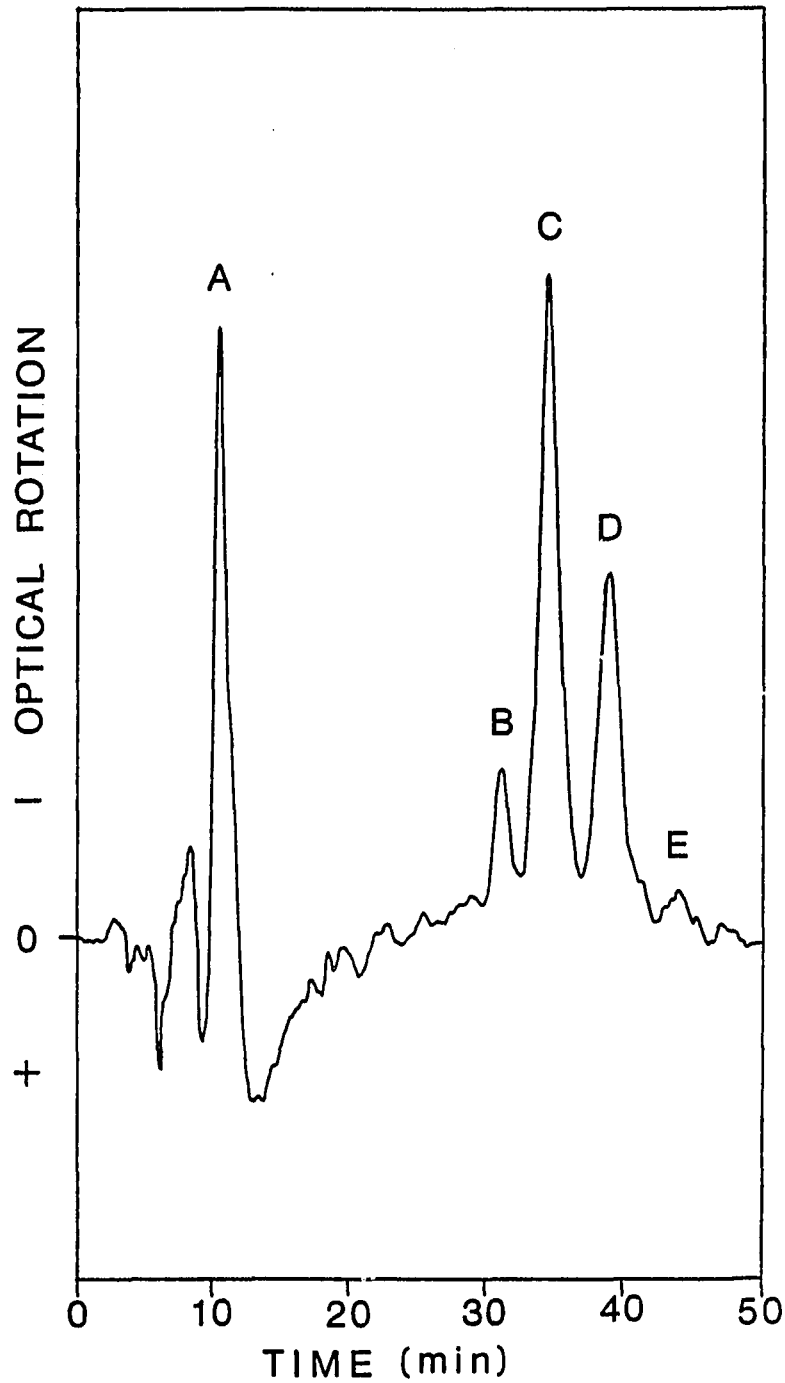
A
B
C
D
E
OPTICAL ROTATION
+
0
0
10
20
30
40
50
TIME (min)

peaks were identified: (A) cholesterol and cholestanol; (B) cholesteryl linolenate and arachidonate; (C) cholesteryl palmitoleate and linoleate; (D) cholesteryl palmitate and oleate; (E) cholesteryl stearate. In general, the order of elution followed that obtained in earlier work using reversed-phase separation (122).

The structural difference between cholesterol and cholestanol is in the presence of an isolated double bond. between carbons 5 and 6. The small structural and molecular weight difference between this pair does not lead to a significant difference in partition coefficient to permit a clean LC separation in our isocratic elution system. The dip (Figure 13) and shoulder (Figure 14) on the descending side of peak A are due to the appearance of cholestanol during the elution of cholesterol. This identification was established by the retention times and the signs of the optical rotations. The large negative rotation of cholesterol ($[\alpha]_D^{20} = -39.5$) (124) was partially offset by the smaller positive rotation of cholestanol ($[\alpha]_D^{22} = +24.2$) (124). A similar situation existed with three other pairs, peak B, C and D. Within each pair, despite the structural difference between the fatty acid chains, the change in polarity still did not manifest sufficient difference in partition coefficients for good separation.

Between the two components in the same peak, the polarity increase due to one additional double bond was effectively offset by the decrease in polarity caused by the existence of two more methylene groups in the fatty acid chain.

Admittedly, the selected experimental conditions did not allow clear separation of every individual component. And, not all the literature values of individual specific rotations, the common detector response factor, are available for the cholesteryl esters. It is still possible to quantitate the combined contribution of those esters. Because the chiral centers are all in the cholesterol part, it is fair to assume similar values for the specific rotations of those cholesteryl esters considering the structural resemblance among them. The identical value of -24 is listed (125) for the specific rotation of cholesteryl palmitate and oleate. We thus take the liberty of using the same value for all components in peak B, C, and D. The calculated serum cholesterol level is shown in Table 2, using the method of triangular approximation discussed earlier.

The percentage of free cholesterol relative to the total amount of cholesterol is within the range of 17-39% reported in previous studies (126, 127). For the purpose of quantitative comparison, an analysis of reference serum (Sigma,

Table 2. Concentration of free and esterified cholesterol in serum

Peak	Compound	Fatty acid[a]	Concentration in serum (mg/dl)[b] Leder Norm	Local
A	Cholesterol Cholestanol		47	38
B	Cholesteryl linolenate Cholesteryl arachidonate	18:3 20:4	7	20
C	Cholesteryl palmitoleate Cholesteryl linoleate	16:1 18:2	76	86
D	Cholesteryl palmitate Cholesteryl oleate	16:0 18:1	56	58
E	Cholesteryl stearate	18:0	8	8
	TOTAL cholesterol		194	210
	Free cholesterol (% of total)		24	18
	Esterified cholesterol (% of total)		76	82

[a]Refers to fatty acid with n carbons and m double bonds.

[b]All concentrations are ±10%.

St. Louis, MO, U.S.A., Cat. No. R3626) was performed. The total cholesterol determined by our HPLC method using optical activity detection was 135 mg/dl. A 130 mg/dl total cholesterol value based on classical Liebermann-Burchard method was provided on the data sheet for this sample. This indicates that our results are at least comparable to that determined colorimetrically. The total serum cholesterol determined by simple summation of the individual cholesterols is well within the normal range of 150 to 250 mg/dl (105).

The fatty acids of cholesterol esters have been separated and quantitated by various chromatographic methods (112). An approximate distribution of the fatty acids of the cholesterol esters of normal serum, expressed as percent of total, is shown in Table 3. The fatty acids of the seven cholesterol esters identified in our work make up about 96% of the total. Assuming the total cholesterol esters determined in this work to be only 96% of the total and calculating the approximate distribution of the cholesterol esters as percent of total accordingly, Table 3 can be constructed for comparison. It is clear that the distribution of the cholesterol esters closely matches that of their corresponding fatty acids detached from the parent esters as expected. With some work, it should be possible to separate peaks B through D into the individual

Table 3. Comparison of the approximate distributions of cholesterol esters and the fatty acids of cholesterol esters

Esterified fatty acid	% of total fatty acid[a]		% of total esters	
			Leder Norm	Local
Linolenic	4	10	5	10
Arachidonic	6			
Palmitoleic	6	49	50	48
Linoleic	43			
Palmitic	10	34	36	33
Oleaic	24			
Stearic	3	3	5	5
Others	4	4	(4)[b]	(4)[b]

[a]From reference [24].

[b]By difference.

components, by for example, introducing silver ions. However, unless future clinical studies show different implications for saturated versus unsaturated cholesterol esters, separation may not be necessary.

One major advantage of optical activity detection is its inherent selectivity. Compounds that do not possess optical activity simply will not interfere with analysis even if they elute with analytes we are interested in. This is especially useful when physiological fluids are being analyzed. Triglycerides were present in serum in relatively high concentrations ranging from 29 to 134 mg/dl (112), and tend to interfere with HPLC serum cholesterol analysis when UV detection was monitored at 200 nm (122). Around 60% of the triglycerides are simple triglycerides (127) which do not possess asymmetric carbon and will elude optical activity detection. Among the 40% mixed triglycerides, only those with different fatty acid substituents on carbons 1 and 3 have the possibility of showing optical rotation since the carbon 2 then becomes asymmetric. Since the majority of the fatty acid substituents come from long chain fatty acids with similar chain lengths, the small structural difference among the three substituents surrounding the asymmetric carbon should only cause insignificant, if any, optical rotation. The combined effect of low optical activity and small quantity in their distribution

make their interference negligible in the region of interest. The numerical results prove this assumption. Small amounts of mono- and diglycerides (less than 2% of the total glycerides (112)) have appreciable polarity because of their free hydroxyl group and were eluted before cholesterol. Also, 7-dehydrocholesterol has been identified in human serum and apparently is present in concentrations ranging from 5 to 40 mg/dl with 20 mg/dl as the median. This optically active compound is a potential interference for free cholesterol. Since about 80% is esterified (24), the spreading of the peaks by gradient elution should greatly reduce its interference. Even as it is, deconvolution techniques can provide individual concentrations for cholesterol and 7-dehydrocholesterol, since the two have retention times that are distinctly different though only slightly. About 1% of total cholesterol is comprised of Δ7-cholesterol, therefore, its interference on free cholesterol is within the possible error estimated in our method. Through the use of a higher efficiency colum and gradient elution, improved separation could be achieved and potential interferences reduced.

In summary, we report here a straightforward procedure for the simultaneous determination of free and esterified cholesterol in human serum. Simple extraction, direct

injection, HPLC and the use of an absolute standard d.c. Faraday cell, offers great convenience in cholesterol determination. The results indicate that this scheme appears to be accurate and precise and to suffer less from interfering substances than colorimetric, enzymatic or UV detection. We expect this technique to be of major importance in the calibration of other analytical methods in clinical studies.

CHAPTER VI. SHALE OIL CHARACTERIZATION BY HPLC AND OPTICAL ACTIVITY DETECTION

Introduction

As a result of increasing demand for liquid hydrocarbons for use both as fuels and as chemical feedstocks and the growing concern regarding the rapid depletion of finite petroleum deposits, an unprecedented push to substitute alternative fossil energy sources for the crude oil is fast picking up momentum. These raw materials for synthetic fuel lie locked in oil shale formations, in coal deposits and gooey tar sands. There, the oil shales are dark-brown, fine-grained sedimentary rocks which were formed as layers of the remains of living organisms were gradually deposited, along with other sediments, in the shallow lakes, marshes, or seas rich in microscopic plant and animal life in many different geological ages (128). The oil shales are rich in organic matter and yield petroleum-like oil when heated to about 500°C (900°F). Although shale oil is generally costlier to produce than is petroleum, it is potentially of great economic importance because there is so much of it.

The Green River Formation located in Colorado, Utah and Wyoming of the United States is the most promising region in the world for shale oil production. This formation

alone contains about 600 billion barrels of recoverable oil trapped in high grade deposits, which are defined to be at least 10 feet thick and to contain 25 or more gallons of oil per ton; this compares with estimated U.S. recoverable petroleum resources of about 500 billion barrels (129). The proper characterization of any fossil fuel, including shale oil, is important to its utilization and to exploration efforts for its reserves. Of the many physical and chemical properties suitable for characterization of shale oil, perhaps the most interesting is the associated optical activity. Optical activity is generally considered to be evidence for biological activity, past or present. Unlike the more reactive functional groups in the molecule, the chiral centers may be retained despite the hostile conditions that led to the formation of fossil fuels. Optically active materials have been found in the montan wax of brown coal (131), oil distillates from coal (132), petroleum distillates (133), lubricating oils (134), and shale oil (135). The observed bulk optical rotation has been correlated with retorting conditions (135), geological source (134), aromatic/aliphatic ratio (133), geological age (133), distillate fraction (136), and thermal history (135). Because of the relatively small amounts of optically active materials that are present, typically very small rotations are observed. And, because of the highly colored

nature of most of these materials, measurements are sometimes impossible to obtain.

It is appropriate to ask the question how significant the bulk optical activity is in any correlation scheme. The reason for this is that optical rotation can be dextrorotatory or levorotatory, and both types have been found in fossil fuels (132). The presence of materials of both classes will cause a cancellation in the observed quantity. The bulk of optical rotation is then only an indication of the minimum amount of chiral materials in the sample. It is, therefore, highly desirable to perform some separation on the sample before the measurement of optical activity. Separation also allows one to determine the individual contributions of the various components to further refine any correlations.

The technique of choice is then liquid chromatography (LC) in conjunction with optical activity detection (78). This new technique has been made possible because of the greatly increased sensitivity offered by laser optics over conventional spectropolarimeters. In applications to studies of carbohydrates in urine (123), and of cholesterol and cholesteryl esters in serum (107), detectabilities are on the order of 100 ng of injected quantity. In terms of actual rotations, this corresponds to angles of the order of

10^{-5} degrees. We can estimate the applicability to shale oil characterization since a bulk value of $[\alpha]_D^{25} = 0.8°$ is typical of these samples (135). To avoid overloading, at most 10 mg of sample can be injected using a standard HPLC column. And, assuming that 20 different chromatographic peaks contribute to the total signal, one can expect the order of 1/2000 of the bulk specific rotation, i.e., 4 x $10^{-4}°$, to be observed for a peak elution volume of 1 mL. This then is within the useful range of the technique.

Experimental

Materials

Various shale oil samples were obtained from the Laramie Energy Research Center, U.S. Department of Energy (Laramie, Wy., U.S.A.). To obtain the saturates, a 0.5 g sample of dried oil was dissolved in 20 mL in cyclohexane. The solution was cooled to 0°C in a circulating cold bath, and 10 mL of 15% phosphorous pentoxide in sulfuric acid was slowly added with stirring. Stirring was continued for 1 hour. The mixture was then transferred and centrifuged for 1/2 hour at 3000 rpm. The cyclohexane layer was drawn off, and the bottom layer was twice more mixed with 10 mL of cyclohexane and centrifuged. The combined solution was then evaporated under nitrogen and weighed. An appropriate

amount of acetonitrile is then used to redissolve the residue under ultrasonic agitation to be used for chromatography. All reagents used were reagent grade material without further purification.

Chromatography

Separation was performed on a 25 cm x 4.6 mm, 10-μm C_{18} column (Alltech, Deerfield, Ill., U.S.A.). Samples were eluted with pure acetonitrile as the mobile phase at a flow rate of 0.8 mL/min. All injections were made through a 200-μL sample loop of a conventional injection valve (Rheodyne, Berkeley, Ca., U.S.A., Model 7010). To reduce any pressure fluctuations caused by the pump (Milton Roy, Riviera Beach, Fla., U.S.A., Model 196-0066-001) at the detector, we used a commercial pulse dampener (Handy and Harman, Norristown, Pa., U.S.A., Model Li-Chroma-Damp II).

Optical activity detection

The basic arrangement for an optical activity detector for LC has been reported earlier (78, 137). In this work, 20 mW of 514 nm radiation from an argon ion laser was used. The flow cell was 10 cm long, with an internal volume of 200 μL. To eliminate the need to provide large currents for modulation in the air-based Faraday rotators, we instead used the eluent in the flow cell as the medium for

polarization modulation. The higher number density of molecules in the liquid versus in the air effectively provides a much larger Faraday effect. Since this is done without introducing additional optical components in the cavity, the favorable extinction ratio is preserved. One can then reduce the current by a factor of 1000, or reduce the number of turns in the solenoid correspondingly. In either case, the electrical power requirement is much lower, thus, shortening the warm-up period. The decrease in inductance in the solenoid also allows higher frequencies to be used in the modulation if desired. It is true that fractional fluctuations in the number and type of molecules in the region of the magnetic field will cause fluctuations in the modulation. However, these are expected to be negligible in our experiments. Application to gradient elution will be difficult, but not impossible, and the air-based Faraday rotators [78] will have to be used instead.

To accomplish the above, we machined the outer core of the flow cell to 1.3 cm o.d. and wound 420 turns of #22 magnetic wire in each of two 2.5 cm long regions (see Figure 17). The two coils are driven in opposing field directions at alternate half-cycles of the modulation by switching transistors. A 10 Ω resistor is put in series with the coils to allow the use of a moderate voltage in the

modulation, since the solenoids have internal resistances of only 1.2 Ω. Using an independent air-based Faraday rotator as before (78), to provide a standard optical rotation, we have determined that the detectability of the system is 1.5×10^{-5}° (S/N = 3) for a time constant of 10 s. For the studies here, a time constant of 3 s was found to be adequate and was used throughout.

Results and Discussion

The chromatograms that are obtained naturally depend heavily on the mode of extraction of the material injected. The particular procedure here is chosen to favor the saturated hydrocarbons, which are known contributors to observed optical activity in fossil fuels. So, although nearly all of the optically active components are found in this fraction in petroleum (138), the situation may be different in shale oil. Also, acetonitrile was chosen as the solvent and the eluent to eliminate the solvent front associated with the injection process. This way, events very early on in the chromatogram can be recorded faithfully. There is, however, no guarantee that all interesting components will be eluted during a run of 40 minutes, or that this choice of eluent/stationary phase is the best. Still, within these guidelines, the studies here provided some

interesting results.

Two different groups of chromatograms are shown in Figures 15 and 16. In Figure 15, the saturates are derived from Anvil Points shale having various particle sizes. Going from bottom to top, the particle sizes are 0-2.5 cm (S-29), 2.5-7.5 cm (S-31), and 7.5-15 cm (S-32). In Figure 16, the saturates all have similar particle sizes (0-2.5 cm) but have different origins and qualities. Going from bottom to top, they represent Utah Shale of 12 gallons/ton (S-34), Anvil Points Shale of 25 gallons/ton (S-29), and Colony Shale of 35 gallons/ton (S-38). To compare these chromatograms properly, one needs to recognize that the vertical scales are somewhat different for each one. Variations in the laser power, optical alignment, electronic gain, and modulation conditions can alter the vertical scale. Fortunately, these can be calibrated using a dc solenoid to produce a known degree of polarization rotation. These instrumental factors result in scale expansions of 1:0.93:0.67 for S-29:S-31:S-32 in Figure 15, and 0.87: 1:0.87 for S-34:S-29:S-38 in Figure 16. Another factor that contributes to the vertical scale is the amount of sample injected for each. Even though the volume injected is held constant, the concentration of material in each changes because of solubility, extraction efficiency,

Figure 15. Chromatograms of shale oil extracts for various particle sizes (S-29, 0-2.5 cm; S-31, 2.5-7.5 cm; S-32, 7.5-15 cm. Vertical scale, see text)

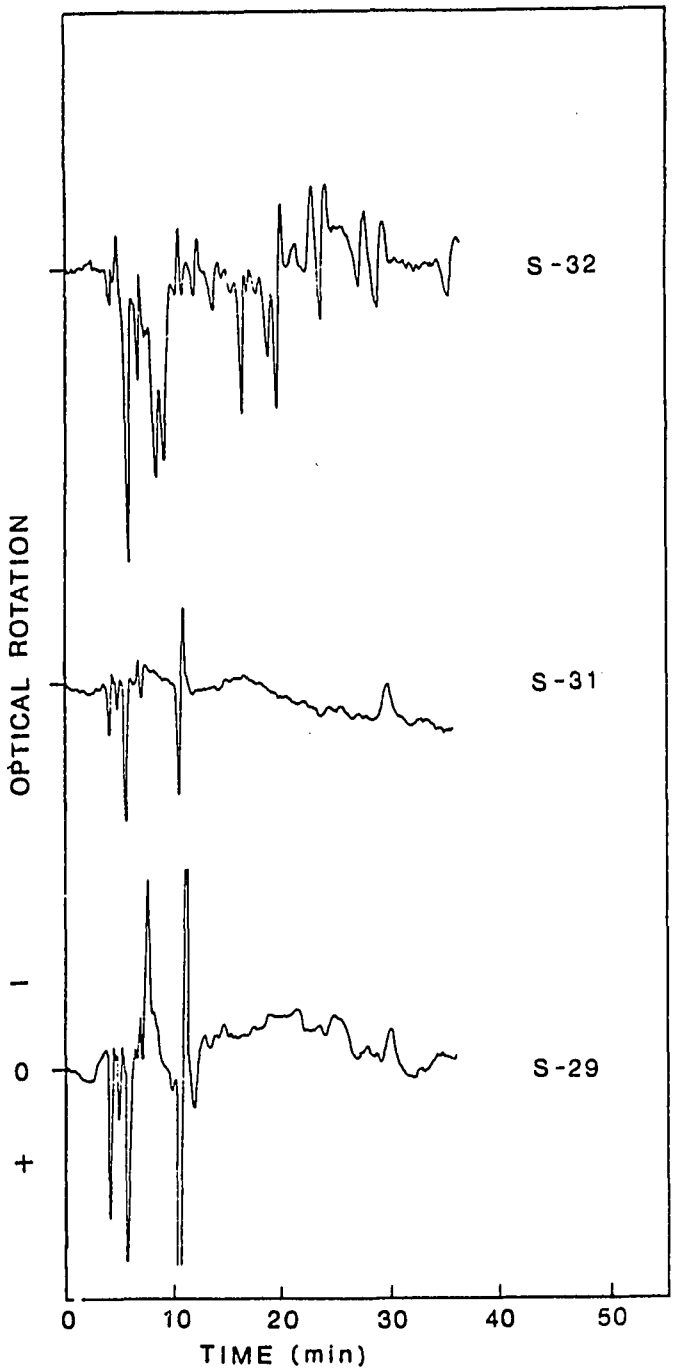
S-32
S-31
S-29
OPTICAL ROTATION
+
0
-
0
10
20
30
40
50
TIME (min)

Figure 16. Chromatograms of shale oil extracts for 0-2.5 cm particle sizes and different origins (S-34, Utah Shale (12 gallons/ton); S-29, Anvil Points Shale (25 gallons/ton); S-38, Colony Shale (35 gallons/ton). Vertical scale, see text)

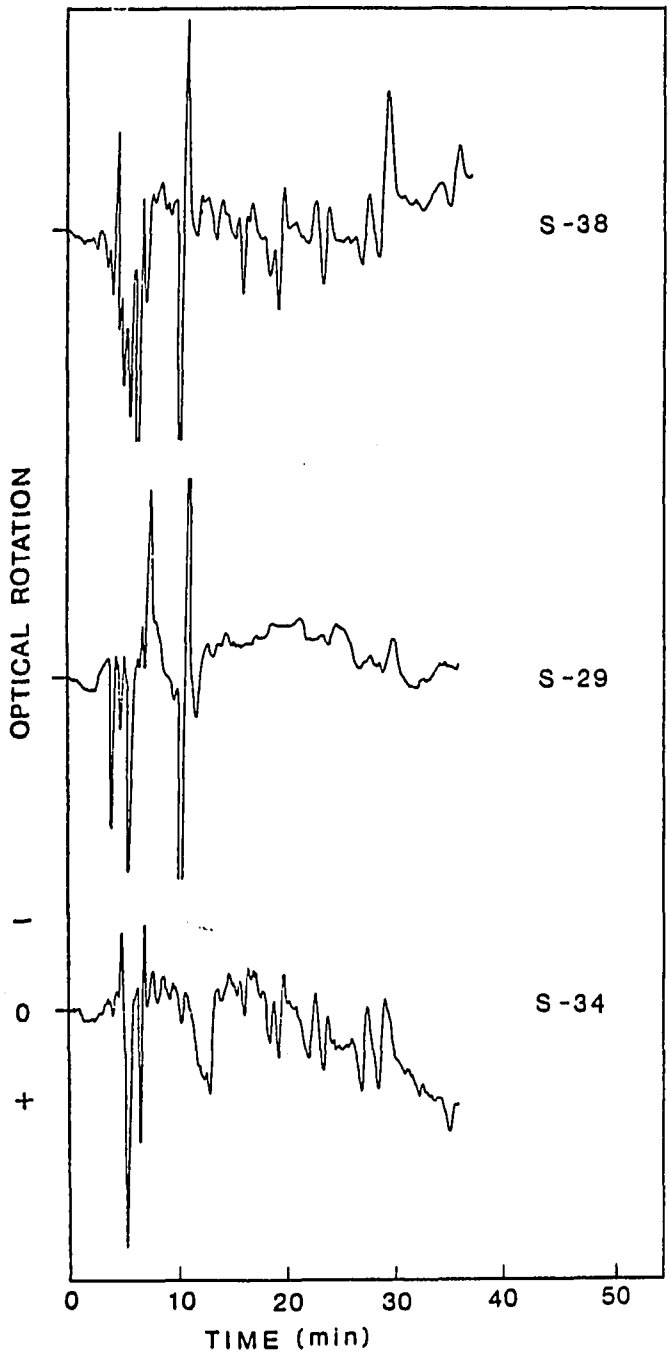
S-38
S-29
S-34
OPTICAL ROTATION
+
0
-
0
10
20
30
40
50
TIME (min)

and dilution factors. A fair assessment of these influences can be obtained by collecting the chromatographic effluent for the entire run, evaporating off the eluent, and then weighing the dry material. This results in a ratio of contents of 10:14:21 for S-29:S-31:S-32 in Figure 15, and a ratio of 20:10:20 for the three in Figure 16. Normalizing with respect to the weight of materials collected and the instrumental factors, one should, therefore, multiply the heights of each peak (from "null") in the chromatograms by 1.0, 0.77 and 0.53 for S-29, S-31 and S-32, respectively, in Figure 15, and by 0.58, 1.0 and 0.58 for S-34, S-29 and S-38, respectively, in Figure 16.

The first observation is that these chromatograms are extremely rich in structure. All chromatograms have been checked with multiple injections, and reproducible results were obtained. There were drifts in the baselines due to the instabilities in the optics and the modulation, but these can be readily distinguished from the chromatographic features. The nature of the instrumentation dictates that any deviation from "null" (baseline) can only be due to an actual rotation of the polarization, and not absorption or refractive index changes. On the other hand, the presence of optically active materials in the chromatographic effluent need not result in a measurable signal due

to possible cancellation of coeluting species. Similarly, the peak heights (from "null") may not be proportional to the concentrations. So, if anything, we may still be underestimating the amount of optically active components in the samples. The second observation is that there are dextrorotatory as well as levorotatory components in all the samples. This confirms that bulk optical activity is not a useful parameter in the characterization of the samples due to cancellation of the effects. In fact, the better the separation, the more reliable is the interpretation. The third observation is that without exception, the integrated optical activity is biased towards the dextrorotatory sense. This is consistent with the measured bulk rotatory powers of these samples (135). It is also consistent with bulk measurements in other types of fossil fuels (132, 133, 136). Presumably the skeletons of certain biological markers are more likely to survive the extreme conditions of fossilization than others, and dominate in the contributions to these measurements. The fourth observation is that the chromatograms show some dependence on the particle sizes of the shale, as illustrated in Figure 15. The chromatograms of the two smaller particle sizes are quite similar, except for a distinctive peak at 7.5 min for the former. The larger particle size, however, provides

more features and quite different relative signal strengths for each. Most notable are additional features at 8, 9, 16, and 19 min, and the absence of a feature at 10 min. Most likely, the larger particles are heated up more slowly because of their mass, and show less cracking and thus more optical activity in the end. Similar observations for various heating rates have been reported in the bulk optical activity (135). The two smaller particle sizes are probably not different enough in mass to show this particular effect. This indicates that uniformly small particles must be used in any studies of correlations. The fifth observation is that there are major differences among samples with different origins. This is most evident in the regions towards the beginning of the chromatograms (to 5 min) and around 12.5 min. Naturally, many more representative samples will have to be surveyed to confirm these trends. The sixth observation is that there are also many similarities among the samples with respect to the location and sign of the chromatographic peaks. If biogenic origin of these shales is accepted, one would expect certain types of chiral skeletons, such as steranes (139), phytane and pristane (140), to be more abundant than others.

In summary, we report here the first chromatograms of the optically active materials in the saturated fraction

of shale oil extract. The wealth of information present suggests that these chromatograms may be good fingerprints of the shale oil, and may be useful for the characterization of fossil fuels in general.

CHAPTER VII. SUMMARY

High performance liquid chromatography (HPLC) has already reached a very high level of sophistication and versatility. The predictions based on the current instrument sales and the intensity of scientific activities show that it will surpass gas chromatography as the major chromatographic technique within a few years. However, chances of developing an ideal LC detector, one that is universal, sensitive, and perhaps even inexpensive, appear to be slim. Besides, a nonselective detector with phenomenal detectability is very likely to yield one large unresolved response when a complex sample matrix is encountered.

An analytical transducer which has response that is more selective to certain classes of compound present great promise in alleviating this problem. This concept has recently been demonstrated through the detection of optically active components in real samples, after separation by HPLC, as described in previous chapters of this thesis.

The attractiveness of monitoring the rotation of plane polarized light by optically active molecules stems primarily from the fact that one can make use of the presence and absence of optical activity, the sign of optical rotation, as well as the wavelength dependence of the rotation, to aid in the identification of chromatographic peaks.

In this work, we have successfully demonstrated the capability of determining submillidegree of optical rotation through the use of our working HPLC optical activity detector. Principles of operation and details of construction of a micropolarimeter have been described in Chapter III. The experimental milestones that have made this possible are the use of selected Glan-Thompson polarizers, selected cell-window material, stable electronic azimuthal modulation based on Faraday effect and the development of a precision optical alignment scheme with which the spectral characteristics of the laser were advantageously incorporated.

The successful practice of this LC detector can be clearly observed through the three specific applications where selectivity is essential to the method development. In human urine, the determination of various sugars, except glucose, has been a problem. The detector based on optical activity is ideal in this case. The detectability of 100 ng allows the simultaneous determination of six naturally occurring carbohydrates, after they are separated by the use of a heavy-metal ion exchange column, in 100-μl samples of human urine. The sample is injected directly except for a simple deionization step. The reproducibility and reliability of this method should allow better insight into the relation between urinary sugars and physiological

conditions.

In human serum, the determination of the lipid profile is of interest. While some success has been reported using far UV absorption, interference between triglycerides and free cholesterol is a problem. Furthermore, important species like cholestanol have no convenient absorption bands. The optical activity detector once again can be used to overcome these problems. For the determination of free, esterified and total cholesterol in human serum, a simple and accurate scheme based on reversed-phase HPLC separation and optical activity detection shows greater advantage over conventional clinical method of analysis.

In the energy-related area, once shale oil is recognized as an indispensable major source of petrochemical feedstock, it becomes increasingly demanding to gain a better understanding of its chemistry, and the characterization of this material is of prime importance. Chromatograms are obtained for various saturated fractions of shale oil, having different particle sizes and from different sources. Separation is accomplished by reversed-phase high-performance liquid chromatography and the eluate is monitored by an optical activity detector. The chromatograms show an abundance of optically active components, which may be good fingerprints for the various shale oils.

REFERENCES

1. Snyder, L. R.; Kirkland, J. J. "Introduction to Modern Liquid Chromatography", 2nd ed.; Wiley-Interscience: New York, 1979.

2. Guiochon, G. Anal. Chem. 1981, 53, 1318.

3. Novotny, M. Anal. Chem. 1981, 53, 1295A.

4. Willard, H. H.: Merritt, L. L. Jr.; Dean, J. A.: Setle, F. A. Jr. "Instrumental Methods of Analysis", 6th ed.; D. Van Nostrand: New York, 1981.

5. DiCesare, J. L.; Ettre, L. S. J. Chromatogr. 1982, 251, 1.

6. McKinely, W. A.; Popovich, D. J.; Layne, T. Amer. Lab. 1980, 8, 37.

7. Parris, N. A. "Instrumental Liquid Chromatography", Elsevier Scientific: Amsterdam, 1976.

8. Yost, R. W.; Ettre, L. S.; Conlon, R. D. "Practical Liquid Chromatography An Introduction"; Perkin-Elmer Corp.: Norwalk, Ct., 1980.

9. Lawrence, J. F. "Organic Trace Analysis by Liquid Chromatography", Academic Press: New York, 1981.

10. Borman, S. A. Anal. Chem. 1982, 54, 327A.

11. Ettre, L. S. J. Chromatogr. Sci. 1978, 16, 396.

12. Majors, R. E.; Barth, H. G.; Lochmuller, C. H. Anal. Chem. 1982, 54, 329R-339R.

13. Ross, M. S. F. J. Chromatogr. 1977, 141, 107.

14. Arpino, P. J.; Guiochon, G. Anal. Chem. 1979, 51, 682A.

15. Schafer, K. H.; Levsen, K. J. Chromatogr. 1981, 206, 245.

16. Griffiths, P. R. In "Transform Techniques in Chemistry", Griffiths, P. R., Ed.; Plenum: New York, 1978.

17. Lowman, D. W. J. Am. Soc. Sugar Beet Technol. 1979, 20, 233.

18. Wright, J. C.; Wirth, M. J. Anal. Chem. 1980, 52, 1087A.

19. Coleman, W. F. Chem. Educ. 1981, 58, 652.; 1982, 59, 441.

20. McKellar, A. R. W.; Oka, T.; Stoicheff, B. P. Eds. "Laser Spectroscopy", Springer-Verlag: Berlin, 1981; Vol. 5.

21. Schawlow, A. L. Science, 1982, 217, 9.

22. Wright, J. C.; Wirth, M. J. Anal. Chem. 1980, 52, 989A.

23. Steinfeld, J. I. CRC Crit. Rev. Anal. Chem. 1975, 6, 225.

24. Omenetto, N.; Winefordner, J. D. CRC Crit. Rev. Anal. Chem. 1981, 12, 59.

25. Omenetto, N., Ed. "Analytical Laser Spectroscopy", John Wiley & Sons: New York, 1979.

26. Hieftje, G. M.; Travis, J. C.; Lytle, F. E., Eds. "Lasers in Chemical Analysis", Humana Press: Clifton, N.J., 1981.

27. Yeung, E. S. In "Lasers in Chemical Analysis", Hieftje, G. M.; Travis, J. C.; Lytle, F. E., Ed.; Humana Press: Clifton, N.J., 1981; Chapter 14.

28. Yeung, E. S. Department of Chemistry, Iowa State University, Ames, Iowa. To be published.

29. Diebold, G. J.; Zare, R. N. Science, 1977, 196, 1439.

30. Himsbey, W. D. III, Milby, K. H.; Zare, R. N. Anal. Chem. 1981, 53, 1509.

31. Sepaniak, M. J.; Yeung, E. S. J. Chromatogr. 1980, 190, 377.

32. Hershberger, L. W.; Callis, J. B.; Christian, G. D. Anal. Chem. 1979, 51, 9.

33. Folestad, S.; Johnson, L.; Josefsson, B. Anal. Chem. 1982, 54, 925.

34. Yeung, E. S.; Sepaniak, M. J. Anal. Chem. 1980, 52, 1465A.

35. Sepaniak, M. J.; Yeung, E. S. Anal. Chem. 1977, 49, 11.

36. Sepaniak, M. J.; Yeung, E. S. J. Chromatogr. 1981, 211, 95.

37. Friedrich, D. M. Chem. Educ. 1982, 59, 472.

38. Huff, P. B.; Tromberg, B. J.; Sepaniak, M. J. Anal. Chem. 1982, 54, 946.

39. Oda, S.; Sawada, T. Anal. Chem. 1981, 53, 471.

40. Dovichi, N. J.; Harris, J. M. Anal. Chem. 1978, 51, 728.

41. Harris, J. M.; Dovichi, N. J. Anal. Chem. 1980, 52, 695A.

42. Leach, R. A.; Harris, J. M. J. Chromatogr. 1981, 218, 15.

43. Freeman, N. K.; Upham, F. T.; Windsor, A. A. Anal. Lett. 1973, 6, 943.

44. Morris, D. M.; Wallen, D. J. Anal. Chem. 1979, 51, 182A.

45. D'Orazio, M.; Schimpf, U. Anal. Chem. 1981, 53, 809.

46. Harvey, A. B. Anal. Chem. 1978, 50, 905A.

47. Carreira, C. A.; Rogers, C. B.; Goss, C. P.; Martin, G. W.; Irwin, R. M.; Wandruszka, R. V.; Berkowitz, D. A. Chem. Biomed. Environ. Instr. 1980, 10, 249.

48. Rogers, L. B.; Sturat, J. D.; Goss, L. P.; Molloy, T. B. Jr.; Carreira, C. A. Anal. Chem. 1977, 49, 958.

49. Woodruff, S. D.; Yeung, E. S. Anal. Chem. 1982, 54, 1174.; to be published.

50. Joregenson, J. W.; Smith, S. L.; Novotny, M. J. Chromatogr. 1977, 142, 233.

51. Voigtman, E.; Jurgensen, A.; Winefordner, J. D. Anal. Chem. 1981, 53, 1921.

52. Hecht, E.; Zajac, A. "Optics", Addison-Wesley: Reading, Mass., 1974.

53. Laitiren, H.; Ewing, G. "A History of Analytical Chemistry"; Maple Press: York, Pa., 1977, p. 165.

54. Morrison, R. T.; Boyd, R. N. "Organic Chemistry", 3rd ed.; Allyn and Bacon: Boston, Mass., 1973; p. 120.

55. O'Loane, J. K. Chem. Rev. 1980, 80, 41.

56. Snelders, H. A. M. J. Chem. Educ. 1974, 51, 2.

57. Buckingham, A. D.; Stiles, P. J. Acct. Chem. Res. 1974, 7, 258.

58. Rosenfeld, L. Z. Phys. 1928, 52, 161.

59. Kirkwood, J. G. J. Chem. Phys. 1937, 5, 479.; 1939, 7, 139.

60. Condon, E. U.; Altar, W.; Eyring, H. J. Chem. Phys. 1937, 5, 753.

61. Mason, S. F. Contemp. Phys. 1968, 9, 239.

62. Caldwell, D. J.; Eyring, H. "The Theory of Optical Activity", Wiley-Interscience: New York, 1971.

63. Clarke, D.; Grainger, J. F. "Polarized light and optical measurement"; Pergamon: Oxford, 1971.

64. Moscowitz, A. In "Optical Rotary Dispersion", Djerassi, C., Ed.; McGraw-Hill: New York, 1960; pp. 151-160.

65. Holum, J. R. "Introduction to Organic and Biological Chemistry", John Wiley & Sons: New York, 1969.

66. Heller, W.; Curme, H. G. In "Physical Methods of Chemistry", Weissberger, A.; Rossiter, B. W. Eds.; Wiley-Interscience: New York, 1972. Vol. 1, Part III.

67. Baumann, A. Z. Anal. Chem. 1977, 284, 31.

68. Rossi, P. Analyst (London), 1975, 100, 25.

69. Drake, A.; Gould, J. M.; Mason, S. F. J. Chromatogr. 1980, 202, 239.

70. Westwood, S. A.; Games, D. E., Sheen, L. J. Chromatogr. 1981, 204, 103.

71. Boehme, W.; Wagner, G.; Oehme, U. Anal. Chem. 1982, 54, 709.

72. Bohme, W. Chromatogr. Newsl. 1980, 8, 38.

73. Skoog, D. A.; West, D. M. "Principle of Instrumental Analysis", Saunder College: Philadelphia, Pa., p. 357.

74. Clarke, D.; Grainger, J. F. "Polarized Light and Optical Measurement", Pergamon Press: Oxford, 1971.

75. O'Shea, D. C.; Callen, W. R.; Rhodes, W. T. "Introduction to Lasers and Their Applications"; Addison-Wesley: Reading, Mass., 1980.

76. "Prism Polarizers". Karl Lambrecht Corp., Chicago, 1980.

77. Moeller, C. E.; Grieser, D. R. Appl. Opt. 1969, 8, 206.

78. Yeung, E. S.; Steenhoek, L. E.; Woodruff, S. D.; Kuo, J. C. Anal. Chem. 1980, 52, 1399.

79. Johnson, E. L.; Stevenson, R. "Basic Liquid Chromatography"; Varian Associates, Inc.: Palo Alto, Ca., 1978, Chapter 11.

80. Olsen, E. D. "Modern Optical Methods of Analysis", McGraw-Hill: New York, 1975.

81. Macek, K. Trends in Anal. Chem. 1981, 1, 35.

82. White, A.; Handler, P.; Smith, E. L. "Principles of Biochemistry", 4th ed.; McGraw-Hill: New York, 1968, p. 842.

83. Juel, R. Amer. J. Clin. Pathol., 1979, 72, 2.

84. Pauling, L. Science, 1968, 160, 268.

85. Burtis, C. A. J. Chromatogr. 1970, 52, 97.

86. Scott, C. D.; Chilcote, D. D.; Katz, S.; Pitt, W. W. Jr., J. Chromatogr. Sci.; 1973, 11, 96.

87. Sharon, N. Scientific American, 1980, 243(5), 90.

88. Sharon, N.; Lis, H. C&EN, 1981, March 30, 21.

89. Davidsohn, I.; Henry, J. B. "Clinical Diagnosis by Laboratory Methods", Saunders: Philadelphia, Pa., 14th ed., 1969, p. 57.

90. Froesch, E. R.; Wolf, H. P.; Baitsch, H. Amer. J. Med., 1963, 34, 151.

91. Lowe, C. U.; Auerback, V. H. In "Textbook of Pediatrics", 8th ed.; Nelson, W. E., Ed.; Saunders, Philadelphia, PA, 1964, p. 298.

92. Freedberg, I. M.; Feingold, D. S.; Hiatt, H. H. Biochem. Biophys. Res. Comm., 1959, 1, 328.

93. Roe, J. H.; Rice, E. W. J. Biol. Chem. 1948, 173, 507.

94. Department of Health, Education and Welfare, and Food and Drug Administration, Fed. Regist., 1974, 39, 24136.

95. Vitek, V.; Vitek, K. Biochem. Med., 1970, 4, 282.

96. Vitek, V., Vitek, K. J. Chromatogr., 1971, 60, 381.

97. Jolley, R. L.; Freeman, M. L. Clin. Chem., 1968, 14, 538.

98. Katz, S.; Dinsmore, S. R.; Pitt, W. W. Jr., Clin. Chem. 1971, 17, 731.

99. Scobell, H. D.; Brobst, K. M.; Steele, E. M. Ceral Chem. 1977, 54, 905.

100. Davies, A. M. C.; Robinson, D. S.; Couchman, R. J. Chemomatogr., 1974, 101, 307.

101. Hyakutake, H.; Hanai, T. J. Chromatogr. 1975, 108, 385.

102. Hughes, S. Ph.D. Dissertation, Iowa State University, Ames, Iowa, 1982.

103. Tietz, N. W., ed. "Fundamentals of Clinical Chemistry", Saunders: Philadelphia, Pa., 1976, Appendix.

104. Brown, M. S.; Goldstein, J. L. Science, 1976, 191, 150.

105. Davidsohn, I.; Henry, J. B., eds. "Todd-Sanford Clinical Diagnosis by Laboratory Methods", 15th ed.; Saunders: Philadelphia, Pa., 1974, pp. 612-639.

106. Gutsche, C. D.; Pasto, D. J. "Fundamentals of Organic Chemistry", Prentice-Hall: Englewood Cliffs, N.J., 1975.

107. Ellefson, R. D.; Caraway, W. T. In "Fundamentals of Clinical Chemistry", Saunders: Philadelphia, Pa., 1976; pp. 506-516.

108. Sabine, J. R. "Cholesterol", Marcel Dekker: New York, 1977.

109. Searcy, R. L. "Diagnostic Biochemistry", McGraw-Hill: New York, 1969.

110. Jungmann, R. A.; Schweppe, J. S. Steroids, 1971, 17, 541.

111. Takeuchi, N.; Yamamura, Y. Atherosclerosis, 1973, 17, 211.

112. Henry, R. J. "Clinical Chemistry Principles and Technica", Harper & Row: New York, 1967.

113. Taylor, R. P.; Broccoli, A. V.; Brisham, C. M. J. Chem. Educ. 1978, 55, 63.

114. Touchstone, J. C.; Murawec, T.; Kasparow, M.; Worthmann W. J. Chromatogr. Sci., 1972, 10, 490.

115. Kritchevsky, D.; Davidson, L. M.; Kim, H. K.; Malhotra, S. Clin. Chem. Acta, 1973, 46, 63.

116. Amenta, J. S. Clin. Chem. 1970, 16, 339.

117. Peter, F.; Reynolds, R. G. J. Chromatogr. 1977, 143, 153.

118. Folch, J.; Lees, M.; Sloane-Stanley. J. Biol. Chem. 1957, 226, 497.

119. Haeffner, E. W.; Hoffmann, C. J. K. J. Chromatogr. 1982, 228, 268.

120. Abell, L. L.; Levy, B. B.; Brodie, B. B.; Kendall, F. E. J. Biol. Chem. 1952, 195, 357.

121. Gambert, P.; Lallemant, C.; Archambault, A.; Maume, B. F.; Padieu, P. J. Chromatogr. 1979, 162, 1.

122. Duncan, I. W.; Culbreth, P. H.; Burtis, C. A. J. Chromatogr., 1979, 162, 281.

123. Kuo, J. C.; Yeung, E. S. J. Chromatogr. 1981, 223, 321.

124. Weast, R. C., ed. "CRC Handbook of Chemistry and Physics", 59th ed.; CRC Press: Boca Raton, Fla., 1978.

125. "1981-1982 Aldrich Catalog Handbook of Fine Chemicals", Aldrich Chemical Co.: Milwaukee, Wi,, 1981.

126. Beuker, H.; Viltkamp, W. A.; Hooghwinkel, G. J. M. Clin. Chim. Acta, 1969, 25, 403.

127. Lindholm, H. Scand. J. Clin. Lab. Invest., Suppl. 1956, 23, 1.

128. Yen, T. F., ed. "Shale Oil, Tar Sands, and Related Fuel Sources", American Chemical Society: Washington, D.C., 1976.

129. Lehninger, A. L. "Biochemistry", 2nd ed.; Worth: New York, 1975.

130. "Exploring Energy Choices", Ford Foundation Energy Policy Project: Washington, D.C., 1974.

131. Jarolim, V.; Streibel, M.; Horak, M.; Sorm, F. Chem. and Indust. 1958, 1142.

132. Zahn, C.; Langer, S. H.; Blaustein, B. D.; Wender, I. Nature 1963, 200, 53.

133. Rosenfeld, W. D. J. Am. Oil Chem. Soc. 1967, 44, 703.

134. Hersh, R. E.; Fenske, M. R.; Matson, H. J.; Koch, E. F.; Booser, E. R.; Braun, W. G. Anal. Chem. 1948, 20, 434.

135. Lawlor, D. L., In "Oil Sands and Oil Shale", Strausz, O. P. Ed., Verlag Chemie: New York, 1978, p. 267.

136. Fenske, M. R.; Carnahan, F. L.; Breston, J. N.; Caser, A. H.; Rescorla, A. R. Ind. Eng. Chem. 1942, 34, 638.

137. Kuo, J. C.; Yeung, E. S. J. Chromatogr. 1982, 229, 293.

138. Oakwood, T. S.; Shriver, D. S.; Fall, H. H.; McAleer, W. J.; Wunz, P. R.; Ind. Eng. Chem. 1952, 44, 2568.

139. Anderson, P. C.; Gardner, P. M.; Whitehead, E. V.; Anders, D. E.; Robinson, W. E. Geochim. Cosmochim. Acta 1969, 33, 1304.

140. Cummins, J. J.; Robinson, W. E. J. Chem. Eng. Data, 1964, 9, 304.

ACKNOWLEDGMENTS

I would like to express my heartfelt appreciation to Dr. Edward S. Yeung who has served as my major professor during my stay at Iowa State University. His technical expertise, patience and perseverance have been the sustaining forces in steering this research project from the inception through the completion. Without his guidance and support, the completion of my graduate program would have been impossible.

I also wish to thank Dr. Steven D. Woodruff for the timely technical assistance he provided during the many phases of this study. His friendship, understanding and generosity will always be remembered.

I also extend my appreciation to my many fellow graduate students who furnished some happy moments that make my life in Ames more enjoyable: Bernie, Don, Bill, Steve, Rob, Carmen, Stan and Juliana. I will especially cherish the companionship that I have shared with my long-time officemate, Bernard Yip.

Thanks are given to my parents, Mr. and Mrs. L. T. Kuo and my wife's parents, Mr. and Mrs. Y. J. Lin for their unfailing love and support.

Last, but not least, I want to express my immense gratitude to my wife, Tsuey-Fen, for the support and under-

standing she has given and shown to me throughout my long career as a graduate student. For her immeasurable contributions to my overall well-being, I am indeed grateful.

APPENDIX

Air-based Faraday Rotator

To construct a 10-cm (or 20-cm) long air-based Faraday rotator (see Figure 17), capable of producing 10^{-3} degrees magnetic rotation, we can first calculate the required magnetic field strength by using the empirical expression discovered by E. Verdet

$$\alpha = V \cdot B \cdot L$$

where α is the angle of rotation in minutes, B is the magnetic field strength in gauss, L is the length in cm of column of the substance which the light traverses, and V is a constant, known as Verdet's constant in (minute)(gauss^{-1})(cm^{-1}), which is characteristic of the substance and is a function of temperature and wavelength (see Table A1).

By convention, a positive Verdet constant corresponds to a (diamagnetic) material for which the Faraday effect is l-rotatory when the light moves parallel to the applied B-field and d-rotatory when it propagages antiparallel to B.

The above formula can be rearranged as

$$B = \frac{\alpha}{V \cdot L}$$

Table A1. Verdet constants for some selected substances[a]

Material	Temperature (°C)	V (minute)(gauss^{-1})(cm^{-1})
Light flint glass	18	0.0317
Water	20	0.0131
NcCl	16	0.0359
Quartz	20	0.0166
$NH_4Fe(SO_4)_2 \cdot 12H_2O$	26	-0.00058
Air[b]	0	6.27×10^{-6}
CO_2	0	9.39×10^{-6}

[a]More extensive listings are given in the usual handbooks.

[b] = 578 nm and 760 nm Hg.

By plugging the following numerical values for the parameters on the right side of the formula,

$$\alpha = 10 \times 10^{-3} \text{ degrees} = 6.0 \times 10^{-2} \text{ minutes}$$

$$V_{air} = 6.27 \times 10^{-6} \text{ (minute)(gauss}^{-1}\text{)(cm}^{-1}\text{)}$$

$$L = 10 \text{ cm}$$

we can obtain a value of 1000 gauss for the necessary magnetic field strength.

The magnetic field strength B in gauss in a long solenoid of n turns per centimeter carrying a current I in ampere is given by the formula

$$B = \frac{4\pi nI}{10}$$

For a field of 1000 gauss with a current of 1 ampere, we found that the solenoid should be wound 800 turns per centimeter for a total of 8000 turns over 10 cm. If a dc current of 0.25 amperes is applied to this air-based Faraday rotator, the angle of rotation produced will be about 2.5×10^{-4} degrees.

Mobile Phase-based Faraday Rotator

In Chapter VI, a mobile phase-based Faraday rotator was constructed (see Figure 17). When water, which possesses a large Verdet constant (0.013 (minute)(gauss^{-1})(cm^{-1}) at 20°C), is chosen as the medium and the

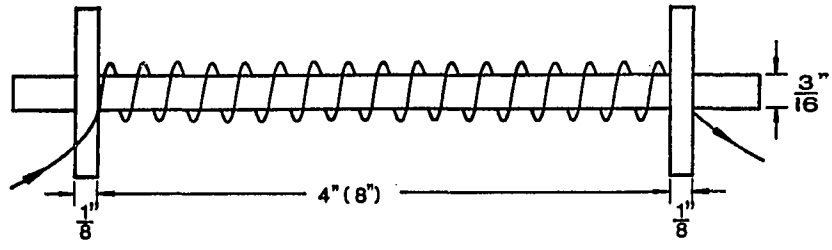

Figure 17a. Air based Faraday rotator

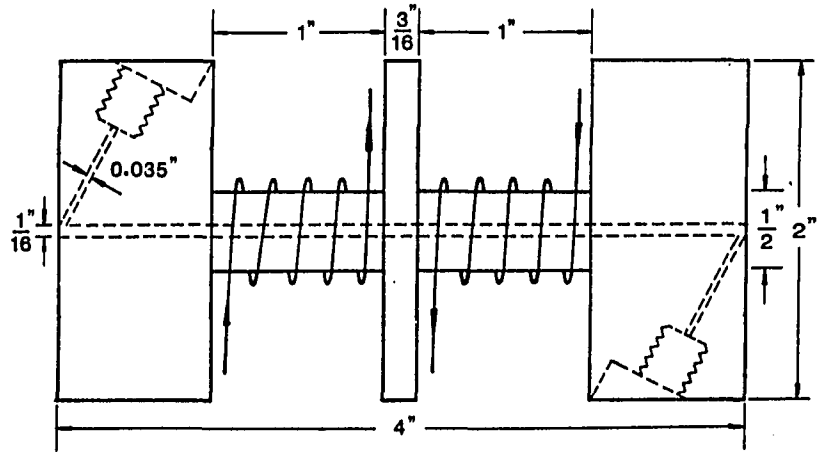

Figure 17b. Mobile-phase based Faraday rotator

Faraday rotator has a length of 2.5 cm, the magnetic field strength needed is then 2 gauss for a magnetic rotation of 1.0×10^{-3} degrees. This translates to a solenoid of about 1.6 turns per centimeter or 4 turns for the 2.5 cm length at 1 ampere dc current. Alternately, we can still increase the number of turns in the solenoid with a corresponding decrease in current consumption and achieve the same effective field strength and magnetic rotation. By winding the solenoid 420 turns per 2.5 cm, we only need to supply a low level current of 10 mA which is well within the capability of commercial dc power supply.